

Geometric Local Variance Gamma model

P. Carr, A. Itkin

*Tandon School of Engineering, New York University,
12 Metro Tech Center, RH 517E, Brooklyn NY 11201, USA*

Abstract

This paper describes another extension of the Local Variance Gamma model originally proposed by P. Carr in 2008, and then further elaborated on by Carr and Nadtochiy, 2017 (CN2017), and Carr and Itkin, 2018 (CI2018). As compared with the latest version of the model developed in CI2018 and called the ELVG (the Expanded Local Variance Gamma model), here we provide two innovations. First, in all previous papers the model was constructed based on a Gamma time-changed *arithmetic* Brownian motion: with no drift in CI2017, and with drift in CI2018, and the local variance to be a function of the spot level only. In contrast, here we develop a *geometric* version of this model with drift. Second, in CN2017 the model was calibrated to option smiles assuming the local variance is a *piecewise constant* function of strike, while in CI2018 the local variance is a *piecewise linear* function of strike. In this paper we consider 3 *piecewise linear* models: the local variance as a function of strike, the local variance as function of log-strike, and the local volatility as a function of strike (so, the local variance is a *piecewise quadratic* function of strike). We show that for all these new constructions it is still possible to derive an ordinary differential equation for the option price, which plays a role of Dupire's equation for the standard local volatility model, and, moreover, it can be solved in closed form. Finally, similar to CI2018, we show that given multiple smiles the whole local variance/volatility surface can be recovered which does not require solving any optimization problem. Instead, it can be done term-by-term by solving a system of non-linear algebraic equations for each maturity which is fast.

Keywords: local volatility, stochastic clock, geometric process, Gamma distribution, piecewise linear volatility, Variance Gamma process, closed form solution, fast calibration, no-arbitrage.

1. Introduction

The Local Variance Gamma (LVG) volatility model was first introduced by P. Carr in 2008 and then presented in Carr and Nadtochiy (2014, 2017) as an extension of the local volatility model by Dupire (1994) and Derman and Kani (1994). The latter was developed on the top of the celebrating

Email addresses: petercarr@nyu.edu (P. Carr), aitkin@nyu.edu (A. Itkin)

Black-Scholes model to take into account the existence of option smile. The main advantage of all local volatility models is that given European options prices or their implied volatilities at points (T, K) where K, T are the option strike and time to maturity, they are able to exactly replicate the local volatility function $\sigma(T, K)$ at these points. This process is called calibration of the local volatility (or, alternatively, implied volatility) surface, see survey in Carr and Itkin (2018); Itkin and Lipton (2018) and references therein.

However, as compared with the classical local volatility model, the LVG and ELVG have several advantages. First, they are richer in the financial sense. Indeed, it is worth noting that the term "local" in the name of the LVG/ELVG models is a bit confusing. This is because, e.g., the ELVG is constructed by equipping an arithmetic Brownian motion with drift and local volatility by stochastic time change $\Gamma_{X(t)}$. Here Γ_t is a Gamma stochastic variable, and $X(t)$ is a deterministic function of time t . As stochastic change is one of the ways of introducing stochastic volatility, it could be observed that the LVG/ELVG is actually a local stochastic volatility (LSV) model which combines local and stochastic features of the volatility process. For more information on the LSV models, see Bergomi (2016); Kienitz and Wetterau (2012).

Another advantage of the LVG/ELVG is that their calibration is computationally more efficient. This is because this construction gives rise not to a partial differential equation (which in the classical case is known as Dupire's equation), but to a partial differential difference equation (PDDE). The latter is actually an ordinary differential equation (ODE) and permits both explicit calibration and fast numerical valuation. In particular, calibration of the local variance surface does not require any optimization method, rather just a root solver, Carr and Itkin (2018).

As discussed in Itkin and Lipton (2018), given the market quotes of European options for various maturities and strikes, the local (and then implied) volatility surface can be obtained by directly solving the Dupire equation using either analytical or numerical methods. The advantage of such an approach is that it guarantees no-arbitrage if the corresponding analytical or numerical method does preserve no-arbitrage (including various interpolations, etc.). Obviously, solving Dupire's PDE requires either numerical methods, e.g. that in Coleman et al. (2001), or, as in Itkin and Lipton (2018), a semi-analytic method which: i) first uses the Laplace-Carson transform, and ii) then applies various transformations to obtain a closed form solution of the transformed equation in terms of Kummer Hypergeometric functions. Still, it requires an inverse Laplace transform to obtain the final solution. To make the second approach tractable, some assumptions should be made about the behavior of the local/implied volatility surface at strikes and maturities where the market quotes are not known. Usually, the corresponding local variance is assumed to be either piecewise constant, Lipton and Sepp (2011), or piecewise linear Itkin and Lipton (2018) in the log-strike space, and piecewise constant in the time to maturity space. A similar assumption is also necessary to make the LVG/ELVG models tractable. In particular, in Carr and Nadtochiy (2017) the model was calibrated to option smiles assuming the local variance is a *piecewise constant* function of strike, while in Carr and Itkin (2018) the local variance is a *piecewise linear* function of strike.

Despite these nice features of the ELVG, one possible problem could be that the model is

developed based on the arithmetic Brownian motion with drift. That means that the underlying, in principle, could acquire negative values, which in some cases is undesirable, e.g., if the underlying is a stock price. Therefore, in this paper we describe another extension of the LVG model which operates with a Gamma time-changed *geometric* Brownian motion with drift, and the local variance which is a function of the spot level only (so is not a function of time).

Second, in Carr and Nadtochiy (2017) the model was calibrated to option smiles assuming the local variance is a *piecewise constant* function of strike, while in Carr and Itkin (2018) the local variance is a *piecewise linear* function of strike. In this paper we consider 3 *piecewise linear* models: the local variance as a function of strike, the local variance as a function of log-strike, and the local volatility as a function of strike (so, the local variance is a *piecewise quadratic* function of strike). We show that in this new model it is still possible to derive an ordinary differential equation for the option price, which plays a role of Dupire's equation for the standard local volatility model. Moreover, in all three cases, this equation can be solved in closed form. Finally, similar to Carr and Itkin (2018) we show that given multiple smiles the whole local variance/volatility surface can be recovered which does not require solving any optimization problem. Instead, it can be done term-by-term, and for every maturity the entire calibration is done by solving a system of non-linear algebraic equations which is significantly faster.

The rest of the paper is organized as follows. In Section 2 the new model, which for an obvious reason we call the Geometric Local Variance Gamma model or the GLVG, is formulated. In Section 3 we derive a forward equation (which is an ordinary differential equation (ODE)) for Put option prices using a homogeneous Bochner subordination approach. Section 4 generalizes this approach by considering the local variance being piecewise constant in time. A closed form solution of the derived ODE is given in terms of Hypergeometric functions for various models of the local variance or volatility. The next Section discusses computation of a source term of this ODE which requires a no-arbitrage interpolation. Using the idea of Itkin and Lipton (2018)), we show how to construct non-linear interpolation which provides both no-arbitrage, and a nice tractable representation of the source term, so that all integrals in the source term can be computed in closed form. In Section 6 calibration of multiple smiles in our model is discussed in detail. To calibrate a single smile we derive a system of nonlinear algebraic equations for the model parameters, and explain how to obtain a smart guess for their initial values. In Section 7 we discuss the results of some numerical experiments where calibration of the model to the given market smiles is done term-by-term. The last Section concludes.

2. Stochastic model

Let W_t be a \mathbb{Q} standard Brownian motion with time index $t \geq 0$. Consider a stochastic process D_t to be a time-homogeneous diffusion with drift μ

$$dD_t = \mu D_t dt + \sigma(D_t) D_t dW_t, \tag{1}$$

where the volatility function σ is local and time-homogeneous.

A unique solution to Eq.(1) exists if $\sigma(D) : \mathbb{R} \rightarrow \mathbb{R}$ is Lipschitz continuous in D and satisfies growth conditions at infinity. Since D is a time-homogeneous Markov process, its infinitesimal generator \mathcal{A} is given by

$$\mathcal{A}\phi(D) \equiv \left[\mu D \nabla_D + \frac{1}{2} \sigma^2(D) D^2 \nabla_D^2 \right] \phi(D) \quad (2)$$

for all twice differentiable functions ϕ . Here ∇_x is a first order differential operator on x . The semigroup of the D process (which here is an expectation under \mathbb{Q}) is

$$\mathcal{T}_t^D \phi(D_t) = e^{t\mathcal{A}} \phi(D_t) = \mathbb{E}_{\mathbb{Q}}[\phi(D_t) | D_0 = D], \quad \forall t \geq 0. \quad (3)$$

This first equality could be also thought of as the Feynman-Kac theorem representation of the solution to the terminal value problem (see, e.g., Lőrinczi et al. (2011)), which connects the expectation in the right hand side to the solution of the corresponding PDE, and then the formal solution of this PDE is given by the exponential operator $e^{t\mathcal{A}}$ applied to the initial condition $\phi(D_t)$.

In the spirit of Carr and Nadtochiy (2017); Carr and Itkin (2018), introduce a new process D_{Γ_t} which is D_t subordinated by the unbiased Gamma clock Γ_t . The density of the unbiased Gamma clock Γ_t at time $t \geq 0$ is

$$\mathbb{Q}\{\Gamma_t \in d\nu\} = \frac{\nu^{m-1} e^{-\nu m/t}}{(t^*)^m \Gamma(m)} d\nu, \quad \nu > 0, \quad m \equiv t/t^*. \quad (4)$$

Here $t^* > 0$ is a free parameter of the process, $\Gamma(x)$ is the Gamma function. It is easy to check that

$$\mathbb{E}_{\mathbb{Q}}[\Gamma_t] = t. \quad (5)$$

Thus, on average the stochastic gamma clock Γ_t runs synchronously with the calendar time t .

As applied to the option pricing problem, we introduce a more complex construction. Namely, consider options written on the underlying process S_t . Without loss of generality and for the sake of clearness let us treat below S_t as the stock price process. Let us define S_t as

$$S_t = D_{\Gamma_{X(t)}} \quad (6)$$

where $X(t)$ is a deterministic function of time t . We need to determine $X(t)$ such that under a risk-neutral measure \mathbb{Q} , the total gains process \hat{S}_t , including the underlying price appreciation and continuous dividends q , after discounting at the risk free rate r is a martingale, see Shreve (1992).

Taking first a derivative of \hat{S}_t

$$d\hat{S}_t = d(e^{-rt} S_t e^{qt}) = e^{(q-r)t} [(q-r)S_t dt + dS_t], \quad (7)$$

and then an expectation of both parts we obtain

$$\mathbb{E}_{\mathbb{Q}}[d(e^{(q-r)t} S_t)] = e^{(q-r)t} \{(q-r)\mathbb{E}_{\mathbb{Q}}[S_t] dt + d\mathbb{E}_{\mathbb{Q}}[S_t]\}. \quad (8)$$

So in order for \hat{S}_t to be a martingale, the RHS of Eq.(8) should vanish. Solving the equation

$$(q - r)y(t)dt + dy(t) = 0, \quad y(t) = \mathbb{E}_{\mathbb{Q}}[S_t|S_s], \quad s < t$$

we obtain

$$\begin{aligned} y(t) &= \mathbb{E}_{\mathbb{Q}}[S_t|S_s] = S_s e^{(r-q)(t-s)}, \\ \mathbb{E}_{\mathbb{Q}}[dS_t|S_s] &= d\mathbb{E}_{\mathbb{Q}}[S_t|S_s] = S_s(r - q)e^{(r-q)(t-s)}. \end{aligned} \quad (9)$$

On the other hand, from Eq.(6)

$$\begin{aligned} \mathbb{E}_{\mathbb{Q}}[dS_t|S_s] &= \mathbb{E}_{\mathbb{Q}}[dD_{\Gamma_{X(t)}}|S_s] = \mu\mathbb{E}_{\mathbb{Q}}[D_{\Gamma_{X(t)}}d\Gamma_{X(t)}|S_s] + \mathbb{E}_{\mathbb{Q}}[\sigma(D_{\Gamma_{X(t)}})D_{\Gamma_{X(t)}}dW_{\Gamma_{X(t)}}|S_s] \\ &= \mu\mathbb{E}_{\mathbb{Q}}[D_{\Gamma_{X(t)}}d\Gamma_{X(t)}|S_s], \end{aligned} \quad (10)$$

because the process $W_{\Gamma_{X(t)}}$ is a local martingale, see Revuz and Yor (1999), chapter 6. Accordingly, the process $W_{\Gamma_{X(t)}}$ inherits this property from W_{Γ_t} , hence $\mathbb{E}_{\mathbb{Q}}[\sigma(D_{\Gamma_{X(t)}})D_{\Gamma_{X(t)}}dW_{\Gamma_{X(t)}}] = 0$.

To proceed, assume the Gamma process Γ_t is independent of W_t (and, accordingly, $\Gamma_{X(t)}$ is independent of $W_{\Gamma_{X(t)}}$). Then the expectation in the RHS of Eq.(10) can be computed, by first conditioning on $\Gamma_{X(t)}$, and then integrating over the distribution of $\Gamma_{X(t)}$ which can be obtained from Eq.(4) by replacing t with $X(t)$, i.e.

$$\begin{aligned} \mathbb{E}_{\mathbb{Q}}[D_{\Gamma_{X(t)}}d\Gamma_{X(t)}|S_s] &= \int_0^\infty \mathbb{E}_{\mathbb{Q}}[D_{\Gamma_{X(t)}}d\Gamma_{X(t)}|\Gamma_{X(t)} = \nu] \frac{\nu^{m-1}e^{-\nu m/X(t)}}{(t^*)^m \Gamma(m)} \\ &= \int_0^\infty \mathbb{E}_{\mathbb{Q}}[D_\nu] \frac{\nu^{m-1}e^{-\nu m/X(t)}}{(t^*)^m \Gamma(m)} d\nu, \quad \nu > 0, \quad m \equiv X(t)/t^*. \end{aligned} \quad (11)$$

The find $\mathbb{E}_{\mathbb{Q}}[D_\nu]$ we take into account Eq.(1) to obtain

$$d\mathbb{E}_{\mathbb{Q}}[D_\nu] = \mathbb{E}_{\mathbb{Q}}[dD_\nu] = \mathbb{E}_{\mathbb{Q}}[\mu D_\nu d\nu + \sigma(D_\nu)D_\nu dW_\nu] = \mu\mathbb{E}_{\mathbb{Q}}[D_\nu]d\nu. \quad (12)$$

Solving this equation with respect to $y(\nu) = \mathbb{E}_{\mathbb{Q}}[D_\nu|D_s]$, we obtain $\mathbb{E}_{\mathbb{Q}}[D_\nu|D_s] = D_s e^{\mu(\nu-s)}$. Since we condition on time s , it means that $D_s = D_{\Gamma_{X(s)}} = S_s$, and thus $\mathbb{E}_{\mathbb{Q}}[D_\nu|D_s] = S_s e^{\mu(\nu-s)}$.

Further, we substitute this into Eq.(11), set the parameter of the Gamma distribution t^* to be $t^* = X(t)$ (so $m = 1$) and integrate to obtain

$$\mathbb{E}_{\mathbb{Q}}[dS_t|S_s] = \mu\mathbb{E}_{\mathbb{Q}}[D_{\Gamma_{X(t)}}d\Gamma_{X(t)}] = S_s e^{-s\mu} \frac{\mu}{1 - \mu X(t)}. \quad (13)$$

Finally, equating representations of $\mathbb{E}_{\mathbb{Q}}[dS_t|S_s]$ obtained in Eq.(9) and Eq.(13) we arrive at the equation for $X(t)$

$$S_0(r - q)e^{(r-q)(t-s)} = S_s e^{-s\mu} \frac{\mu}{1 - \mu X(t)}. \quad (14)$$

Assuming $\mu = r - q$, this equation can be solved to provide

$$X(t) = \frac{1 - e^{-(r-q)t}}{r - q}. \quad (15)$$

This expression for $X(t)$ was also used in Carr and Itkin (2018) for the ELVG. We already mentioned that the ELVG could be considered as an *arithmetic analog* of our model in this paper, which is *geometric* in D_t .

It is clear that in the limit $r \rightarrow 0$, $q \rightarrow 0$ we have $X(t) = t$. Also based on Eq.(5)

$$\mathbb{E}_{\mathbb{Q}}[\Gamma_{X(t)}] = X(t). \quad (16)$$

Function $X(t)$ starts at zero, i.e. $X(0) = 0$ ¹, and is a continuous non-decreasing function of time t . In more detail, if $r - q > 0$, function $X(t)$ is increasing in t in all points except at $t \rightarrow \infty$, where it tends to constant. However, the infinite time horizon doesn't have much practical sense, therefore for any finite time t function $X(t)$ can be treated as an increasing function in t . In the other case when $r - q < 0$, function $X(t)$ is strictly increasing $\forall t \in [0, \infty)$. This means that, overall, $X(t)$ has all properties of a good clock. Accordingly, $\Gamma_{X(t)}$ has all properties of a random time.

Thus, we managed to demonstrate that with this choice of μ and $X(t)$ the right hands part of Eq.(8) vanishes, and our discounted stock process with allowance for non-zero interest rates and continuous dividends becomes a martingale. So the proposed construction can be used for option pricing.

This setting can be easily generalized for time-dependent interest rates $r(t)$ and continuous dividends $q(t)$. We leave it for the reader.

The next step is to establish a connection between the original and time-changed processes. It is known from Bochner (1949) that the process G_{Γ_t} defined as

$$dG_t = \sigma^2(G)G_t dW_t$$

is a time-homogeneous Markov process. Same is true for the process $(r - q)G_t dt$. Thus, the entire process D_t defined in Eq.(1) is also a time-homogeneous Markov process. Accordingly, the semigroups T_t^S of S_t and T_t^D of $D_{\Gamma_{X(t)}}$ are connected by the Bochner integral²

$$\mathcal{T}_t^S U(S) = \int_0^\infty \mathcal{T}_\nu^D U(S) \mathbb{Q}\{\Gamma_{X(t)} \in d\nu\}, \quad \forall t \geq 0, \quad (17)$$

where $U(S)$ is a function in the domain of both \mathcal{T}_t^D and \mathcal{T}_t^S . It can be derived by exploiting the time homogeneity of the D process, conditioning on the gamma time first, and taking into account the independence of Γ_t and W_t (or $\Gamma_{\Gamma_{X(t)}}$ and $W_{\Gamma_{X(t)}}$ in our case).

¹So our assumption made in above that $X(0) = 0$ is consistent.

²Here it represents an expectation of the option price with respect to the second stochastic driver - stochastic clock ν .

As we set parameter t^* of the gamma clock to $t^* = X(t)$, Eq.(17) and Eq.(4) imply

$$\mathcal{T}_t^S U(S) = \int_0^\infty \mathcal{T}_\nu^D U(S) \frac{e^{-\nu/X(t)}}{X(t)} d\nu. \quad (18)$$

In what follows for the sake of brevity we call this model as the Geometric Local Variance Gamma model, or the GLVG.

3. Forward equation for option prices

In this section we derive a forward equation for put option prices, which is an analog of the Dupire equation for the standard local volatility model. In doing so, we closely follow the description in the corresponding section of Carr and Itkin (2018), as from the derivation point of view the GLVG differs from the ELVG just by the definitions of infinitesimal generator \mathcal{A} of the process D_t .

Let us interpret the index t of the semigroup \mathcal{T}_t^S as the maturity date T of an European claim with the valuation time $t_v = 0$. Also let the test function $U(S)$ be the payoff of this European claim, i.e.

$$U(S_T) = e^{-rT}(K - S_T)^+. \quad (19)$$

Then define

$$P(S_0, T, K) = \mathcal{T}_T^S U(S_0) \quad (20)$$

as the European Put value with maturity T at time $t = 0$ in the LVGE model. Similarly

$$P^D(S_0, \nu, K) = \mathcal{T}_\nu^D U(S_0) \quad (21)$$

would be the European Put value with maturity ν at time $t = 0$ in the model of Eq.(1)³. Then the Bochner integral in Eq.(18) takes the form

$$P(S, T, K) = \int_0^\infty P^D(S, \nu, K) p e^{-p\nu} d\nu, \quad p \equiv 1/X(T). \quad (22)$$

Thus, $P(S, T, K)$ is represented by a Laplace-Carson transform of $P^D(S, \nu, K)$ with p being a parameter of the transform. Note that

$$P(S, 0, K) = P^D(S, 0, K) = U(S). \quad (23)$$

To proceed, we need an analog of the Dupire forward PDE for $P^D(S, \nu, K)$.

³Below for simplicity of notation we drop the subscript '0' in S_0 .

3.1. Dupire-like forward PDE

Despite this can be done in many different ways, below for the sake of compatibility we do it in the spirit of Carr and Nadtochiy (2017).

First, differentiating Eq.(21) by ν with allowance for Eq.(3) yields

$$\nabla_\nu P^D(S, \nu, K) = e^{-r\nu} e^{\nu\mathcal{A}} [\mathcal{A} - r] U(S) = e^{-r\nu} \mathbb{E}_\mathbb{Q} [\mathcal{A} - r] U(S). \quad (24)$$

We take into account the definition of the generator \mathcal{A} in Eq.(2), and also remind that at $t = 0$ we have $D_0 = S_0 \equiv S$. Then Eq.(24) transforms to

$$\nabla_\nu P^D(S, \nu, K) = -rP^D(S, \nu, K) + (r - q)S\nabla_S P^D(S, \nu, K) + e^{-r\nu} \frac{1}{2} \mathbb{E}_\mathbb{Q} [\sigma^2(S)S^2\nabla_S^2 U(S)]. \quad (25)$$

However, we need to express the forward equation using a pair of independent variables (ν, K) while Eq.(24) is derived in terms of (ν, S) . To do this, observe that

$$\begin{aligned} \mathbb{E}_\mathbb{Q} [\sigma^2(S)S^2\nabla_S^2 U(S)] &= \mathbb{E}_\mathbb{Q} [\sigma^2(S)S^2\delta(K - S)] = \mathbb{E}_\mathbb{Q} [\sigma^2(K)K^2\delta(K - S)] \\ &= \mathbb{E}_\mathbb{Q} [\sigma^2(K)K^2\nabla_K^2 U(S)] = e^{r\nu} \sigma^2(K)\nabla_K^2 P^D(S, \nu, K). \end{aligned} \quad (26)$$

where the sifting property of the Dirac delta function $\delta(S - K)$ has been used. Also

$$\begin{aligned} &-rP^D(S, \nu, K) + (r - q)S\nabla_S P^D(S, \nu, K) \\ &= e^{-r\nu} \mathbb{E}_\mathbb{Q} \left[-r(K - S)^+ + (r - q)S \frac{\partial(K - S)^+}{\partial S} \right] \\ &= e^{-r\nu} \mathbb{E}_\mathbb{Q} \left[-r(K - S)^+ - (r - q)(K - S) \frac{\partial(K - S)^+}{\partial S} + (r - q)K \frac{\partial(K - S)^+}{\partial S} \right] \\ &= e^{-r\nu} \mathbb{E}_\mathbb{Q} \left[-r(K - S)^+ + (r - q)(K - S)^+ - (r - q)K \frac{\partial(K - S)^+}{\partial K} \right] \\ &= -qP^D(S, \nu, K) - (r - q)K\nabla_K P^D(S, \nu, K). \end{aligned} \quad (27)$$

Therefore, using Eq.(26) and Eq.(27), Eq.(24) could be transformed to

$$\begin{aligned} \nabla_\nu P^D(S, \nu, K) &= -qP^D(S, \nu, K) - (r - q)K\nabla_K P^D(S, \nu, K) + \frac{1}{2} \sigma^2(K)K^2\nabla_K^2 P^D(S, \nu, K) \\ &\equiv \mathcal{A}^K P^D(S, \nu, K), \\ \mathcal{A}^K &= -q - (r - q)K\nabla_K + \frac{1}{2} \sigma^2(K)K^2\nabla_K^2. \end{aligned} \quad (28)$$

This equation looks exactly like the Dupire equation with non-zero interest rates and continuous dividends, see, e.g., Ekström and Tysk (2012) and references therein. Note, that \mathcal{A}^K is also a time-homogeneous generator.

3.2. PDDE for a single term

Our final step is to apply the linear differential operator \mathcal{L} defined in Eq.(28) to both parts of Eq.(22). Using time-homogeneity of D_t and again the Dupire equation Eq.(28), we obtain

$$\begin{aligned}
& -qP(S, T, K) - (r - q)K\nabla_K P(S, T, K) + \frac{1}{2}\sigma^2(K)K^2\nabla_K^2 P(S, T, K) \\
&= \int_0^\infty pe^{-p\nu} \left[-qP^D(S, \nu, K) - (r - q)K\nabla_K P^D(S, \nu, K) + \frac{1}{2}\sigma^2(K)K^2\nabla_K^2 P^D(S, \nu, K) \right] d\nu \\
&= \int_0^\infty pe^{-p\nu} \nabla_\nu P^D(S, \nu, K) d\nu = -pP^D(S, 0, K) + p \int_0^\infty P^D(S, \nu, K) pe^{-p\nu} d\nu \\
&= p [P(S, T, K) - P^D(S, 0, K)] = p [P(S, T, K) - P(S, 0, K)],
\end{aligned} \tag{29}$$

where in the last line we took into account Eq.(23).

Thus, finally $P(S, T, K)$ solves the following problem

$$\begin{aligned}
& -qP(S, T, K) - (r - q)K\nabla_K P(S, T, K) + \frac{1}{2}\sigma^2(K)K^2\nabla_K^2 P(S, T, K) = \frac{P(S, T, K) - P(S, 0, K)}{X(T)}, \\
& P(S, 0, K) = (K - S)^+.
\end{aligned} \tag{30}$$

In contrast to the Dupire equation which belongs to the class of PDE, Eq.(30) is an ODE, or more precisely a partial divided-difference equation (PDDE), since the derivative in time in the right hands part is now replaced by a divided difference. In the form of an ODE it reads

$$\left[\frac{1}{2}\sigma^2(K)K^2\nabla_K^2 - (r - q)K\nabla_K - \left(q + \frac{1}{X(T)} \right) \right] P(S, T, K) = -\frac{P(S, 0, K)}{X(T)}. \tag{31}$$

This equation could be solved analytically for some particular form of the local volatility function $\sigma(K)$ which are considered in the next Section. Also in the same way a similar equation could be derived for the Call option price $C_0(S, T, K)$ which reads

$$\begin{aligned}
& \left[\frac{1}{2}\sigma^2(K)K^2\nabla_K^2 + (r - q)K\nabla_K - \left(q + \frac{1}{X(T)} \right) \right] C_0(S, T, K) = -\frac{C_0(S, 0, K)}{X(T)}, \\
& C_0(S, 0, K) = (S - K)^+.
\end{aligned} \tag{32}$$

Solving Eq.(31) or Eq.(32) provides the way to determine $\sigma(K)$ given market quotes of Call and Put options with maturity T . However, this allows calibration of just a single term. Calibration of the entire local volatility surface, in principle, could be done term-by-term (because of the time-homogeneity assumption) if Eq.(31), Eq.(32) could be generalized to this case.

3.3. PDDE for multiple terms

This generalization can be done in the same way as presented in Carr and Itkin (2018), Section 4. Therefore, we refer the reader to that Section while here provide just some useful comments.

To address calibration of multiple smiles we need to relax the assumption about time-homogeneity of the D_t process defined in Eq.(1). We assume that the local variance $\sigma(D_t)$ is no more time-homogeneous, but a piecewise constant function of time $\sigma(D_t, t)$.

Let T_1, T_2, \dots, T_M be the time points at which the variance rate $\sigma^2(D_t)$ jumps deterministically. In other words, at the interval $t \in [T_0, T_1)$, the variance rate is $\sigma_0^2(D_t)$, at $t \in [T_1, T_2)$ it is $\sigma_1^2(D_t)$, etc. This can be also represented as

$$\begin{aligned}\sigma^2(D_t, t) &= \sum_{i=0}^M \sigma_i^2(D_t) w_i(t), \\ w_i(t) &\equiv \mathbf{1}_{t-T_i} - \mathbf{1}_{t-T_{i+1}}, \quad i = 0, \dots, M, \quad T_0 = 0, \quad T_{M+1} = \infty.\end{aligned}\tag{33}$$

Note, that

$$\sum_{i=0}^M w_i(t) = \mathbf{1}_t - \mathbf{1}_{t-\infty} = 1, \quad \forall t \geq 0.$$

Therefore, in case when all $\sigma_i^2(D_t)$ are equal, ie, independent on index i , Eq.(33) reduces to the case considered in the previous Sections.

This implies that the volatility $\sigma(D_t)$ jumps as a function of time at the calendar times T_0, T_1, \dots, T_M , and not at the business times ν determined by the Gamma clock. Otherwise, the volatility function would have been changed at random (business) times which means it is stochastic. But this definitely lies out of scope of our model. Therefore, we need to change Eq.(33) to

$$\sigma^2(D_t, t) = \sum_{i=0}^M \sigma_i^2(D) \bar{w}_i(\mathbb{E}_{\mathbb{Q}}(t)),\tag{34}$$

$$\begin{aligned}\bar{w}_i(\mathbb{E}_{\mathbb{Q}}(t)) &= \mathbf{1}_{X^{-1}(t-T_i)} - \mathbf{1}_{X^{-1}(t-T_{i+1})}, \quad i = 0, \dots, M, \\ X^{-1}(t) &= \frac{1}{q-r} \log [1 - (r-q)t].\end{aligned}\tag{35}$$

As per the last line, $X(t)$ exists $\forall t \geq 0$ if $q > r$, and $\forall t < 1/(r-q)$ if $r > q$.

Hence, when using Eq.(6) we have

$$\sigma^2(D_t, t) \Big|_{t=\Gamma_{X(t)}} = \sum_{i=0}^M \sigma_i^2(D) \bar{w}_i(X(t)) = \sum_{i=0}^M \sigma_i^2(D) w_i(t).\tag{36}$$

Accordingly, if the calendar time t belongs to the interval $T_0 \leq t < T_1$, the infinitesimal generator \mathcal{A} of the semigroup \mathcal{T}_{ν}^D is a function of $\sigma(D_t)$ (and not on $\sigma(D_{\nu})$). As at $T_0 \leq t < T_1$ we assume

$\sigma(D) = \sigma_0(D)$, i.e. is constant in time, it doesn't depend of ν . Thus, \mathcal{A} (which for this interval of time we will denote as \mathcal{A}_0) is still time-homogeneous.

Similarly, one can see, that for $T_1 \leq t < T_2$ the infinitesimal generator \mathcal{A}_1 of the semigroup \mathcal{T}_ν^D is also time-homogeneous and depends on $\sigma_1(D)$, etc.

Further, similar to Carr and Itkin (2018) it could be shown that the forward partial divided difference equation for the Put price $P(S, T_i, K)$, $i = 1, \dots, M$ reads

$$\left[\frac{1}{2} \sigma^2(K) K^2 \nabla_K^2 - (r - q) K \nabla_K - \left(q + \frac{1}{X(T_i) - X(T_{i-1})} \right) \right] P(S, T_i, K) = - \frac{P(S, T_{i-1}, K)}{X(T_i) - X(T_{i-1})}. \quad (37)$$

Here the local variance function $\sigma^2(K) = \sigma_i^2(K)$ as it corresponds to the interval $(T_{i-1}, T_i]$ where the above ODE is solved.

Eq.(37) is a recurrent equation that can be solved for all $i = 1, \dots, M$ sequentially starting with $i = 1$ subject to some boundary conditions.

3.4. Boundary conditions

In many financial models where dynamics of the stock price is represented by a geometric Brownian motion (perhaps with local or stochastic volatility), for instance, the celebrated Black-Scholes model, the boundary condition at $K \rightarrow \infty$ is set to be

$$P(S, T_i, K) \rightarrow \mathcal{D}_i K - \mathcal{Q}_i S, \quad K \rightarrow \infty,$$

where $\mathcal{D}_i = e^{-rT_i}$ is the discount factor, and $\mathcal{Q}_i = e^{-qT_i}$. Indeed, as it could be easily checked this condition is a valid solution of the Dupire forward equation Eq.(28), and also reflects the fact that at $K \rightarrow \infty$ the Put option price should be linear in K . However, this boundary condition doesn't solve Eq.(31), so it could not be used in our model.

Therefore, we propose to setup the boundary condition at $K \rightarrow \infty$ by still assuming it to be a linear function of K of the form

$$\lim_{K \rightarrow \infty} P(S, T, K) = A(T)K - B(T)S, \quad (38)$$

where $A(T), B(T)$ are some functions of maturity T to be determined, so the expression in Eq.(38) solves Eq.(31).

Obviously, $T_0 = 0$ implies $A(T_0) = B(T_0) = 1$. Then we can proceed recursively. For the next given maturity $T = T_1$ plugging in Eq.(38) into Eq.(37) we obtain at $K \rightarrow \infty$

$$\begin{aligned} -(r - q)KA(T_1)p_1 - (p_1q + 1)(A(T_1)K - B(T_1)S) &= -P(S, T_0, K), \\ P(S, T_0, K) &= A(T_0)K - B(T_0)S = K - S, \\ p_j &= X(T_j) - X(T_{j-1}) > 0. \end{aligned} \quad (39)$$

From these equations we obtain

$$B(T_1) = \frac{1}{p_1q + 1}, \quad A(T_1) = \frac{1}{p_1r + 1}. \quad (40)$$

So in this case $A(T_1), B(T_1)$ are an analog of some kind of discrete compounding.

Proceeding recursively, we derive a general relationship

$$\begin{aligned} B(T_i) &= \frac{B(T_{i-1})}{p_iq + 1} = \frac{1}{\prod_{k=1}^i (p_kq + 1)}, \\ A(T_i) &= \frac{A(T_{i-1})}{p_ir + 1} = \frac{1}{\prod_{k=1}^i (p_kr + 1)}, \quad i = 1, \dots, M. \end{aligned} \quad (41)$$

Therefore, in our model the natural boundary conditions for the Put option price are

$$\begin{cases} P(S, T_i, K) = 0, & K \rightarrow 0, \\ P(S, T_i, K) = A(T_i)K - B(T_i)S \approx A(T_i)K, & K \rightarrow \infty, \end{cases} \quad (42)$$

A similar equation can be obtained for the Call option prices, which reads

$$\left[\frac{1}{2} \sigma^2(K) K^2 \nabla_K^2 + (r - q) K \nabla_K - \left(q + \frac{1}{X(T_i) - X(T_{i-1})} \right) \right] C(S, T_i, K) = - \frac{C(S, T_{i-1}, K)}{X(T_i) - X(T_{i-1})}. \quad (43)$$

subject to the boundary conditions

$$\begin{cases} C(S, T_i, K) = B(T_i)S, & K \rightarrow 0, \\ C(S, T_i, K) = 0, & K \rightarrow \infty. \end{cases} \quad (44)$$

4. Piecewise models of local variance/volatility

To calibrate the local volatility surface by solving Eq.(37) we need to make further assumptions about the shape of the local volatility surface. To recall, we assume this surface to be piecewise constant in time. In the strike space Carr and Nadtochiy (2017) considered it to be a piecewise constant, while in Carr and Itkin (2018) a piecewise linear local variance in the strike space was considered. As shown in Carr and Itkin (2018) in that cases Eq.(37) can be solved in closed form.

In this paper we want to extend a class of local volatility models that allow a closed form solution. To proceed, we start by doing a change of the dependent variable from $P(S, T_j, K)$ to

$$V(S, T_j, K) = P(S, T_j, K) - [A(T_j)K - B(T_j)S]^+, \quad (45)$$

where V is known as a *covered Put*. This definition of V allows re-writing Eq.(37) in a more elegant form

$$\begin{aligned} -v_j(x)x^2V_{x,x}(x) + b_{1,j}xV_x(x) + b_{0,j}V(x) &= c_j(x), \\ b_{1,j} = p_j(r - q), \quad b_{0,j} = p_jq + 1, \quad c_j(x) = V(S, T_{j-1}, x), \quad v_j(x) &= p_j\sigma^2(x)/2, \end{aligned} \quad (46)$$

where $V(x) = V(S, T_j, x)$ and $x = K/S$ is the inverse moneyness.

Accordingly, based on the definition of $V(x)$ and Eq.(42), the boundary conditions to Eq.(46) become homogeneous

$$\begin{cases} V(x) = 0, & x \rightarrow 0, \\ V(x) = 0, & x \rightarrow \infty. \end{cases} \quad (47)$$

In the next sections we consider several popular approximations of the local volatility surface in the strike space. Each approximation assumes some functional form of the local volatility curve in the strike space, which is a strip of the volatility surface given time to maturity T . Thus, parameters of these approximations change with time. Also further on for the sake of certainty we assume that $r > q > 0$, but this assumption could be easily relaxed.

4.1. Local variance piecewise linear in a log-strike space

Suppose that for each maturity T_j , $j \in [1, M]$ the market quotes are provided for a set of strikes $K_i, i = 1, \dots, n_j$ where these strikes are assumed to be sorted in the increasing order. Then the corresponding continuous piecewise linear local variance function $\sigma_j^2(\chi)$ at the interval $[\chi_i, \chi_{i+1}]$, $\chi = \log K_i/S$, reads

$$v_{j,i}(\chi) = v_{j,i}^0 + v_{j,i}^1\chi. \quad (48)$$

Here we use the super-index 0 to denote a level v^0 , and the super-index 1 to denote a slope v^1 . Subindex $i = 0$ in $v_{j,0}^0, v_{j,0}^1$ corresponds to the interval $(0, \chi_1]$. Since $v_j(\chi)$ is a continuous function in χ , we have

$$v_{j,i}^0 + v_{j,i}^1\chi_{i+1} = v_{j,i+1}^0 + v_{j,i+1}^1\chi_{i+1}, \quad i = 0, \dots, n_j - 1. \quad (49)$$

This means that the first derivative of $v_j(\chi)$ experiences a jump at points χ_i , $i \in Z \cap [1, n_j]$. As we assumed that $v(\chi, T)$ is a piecewise constant function of time, $v_{j,i}^0, v_{j,i}^1$ do not depend on T at the intervals $[T_j, T_{j+1})$, $j \in [0, M - 1]$, and jump to the new values at the points T_j , $j \in Z \cap [1, M]$.

A simple analysis shows that under this assumption by making a change of variables $x \mapsto \chi$, Eq.(46) could be transformed to

$$-v(\chi)V_{\chi,\chi}(\chi) + (b_1 + v(\chi))V_\chi(\chi) + b_0V(\chi) = c(\chi), \quad (50)$$

where for simplicity of notation we dropped index j .

This equation has the same type as that considered in Itkin and Lipton (2018), Section 2, and its solution could also be expressed in terms of confluent Hypergeometric functions, see Polyanin and Zaitsev (2003)

$$\begin{aligned} V(\chi) &= C_1 y_1(\chi) + C_2 y_2(\chi) + I_{12}(\chi) \\ I_{12}(\chi) &= y_2(\chi) \int \frac{y_1(\chi)c(\chi)}{(b_2 + a_2\chi)W} d\chi - y_1(\chi) \int \frac{y_2c(\chi)}{(b_2 + a_2\chi)W} d\chi, \end{aligned} \quad (51)$$

where $W = y_1(y_2)_\chi - y_2(y_1)_\chi$ is the so-called Wronskian of the fundamental solutions y_1, y_2 . Thus, the problem is reduced to finding suitable fundamental solutions of the homogeneous version of Eq.(51). Based on Polyanin and Zaitsev (2003), if $a_2 \neq 0$ and $a_0 \neq 0$, the general solution reads

$$\begin{aligned} V(\chi) &= (a_2 z)^{\beta_1 - 1} \mathcal{J}(\alpha_1, \beta_1, z), \\ z &= \chi + \frac{b_2}{a_2}, \quad \alpha_1 = 1 + \frac{b_0 + b_1}{a_2}, \quad \beta_1 = 2 + \frac{b_1}{a_2}. \end{aligned} \quad (52)$$

Here $\mathcal{J}(a, b, z)$ is an arbitrary solution of the degenerate Hypergeometric equation, i.e., Kummer's function, Abramowitz and Stegun (1964). Two types of Kummer's functions are known, namely $M(a, b, z)$ and $U(a, b, z)$, which are Kummer's functions of the first and second kind ⁴.

Accordingly, the approach of Itkin and Lipton (2018) can be directly applied to obtain a closed form solution of Eq.(51). In particular, in the vicinity of the origin the numerically satisfactory pair is, Olver (1997)

$$\begin{aligned} y_1(\chi) &= (a_2 z)^{\beta_1 - 1} M(\alpha_1, \beta_1, z), \\ y_2(\chi) &= (a_2)^{\beta_1 - 1} M(\alpha_1 - \beta_1 + 1, 2 - \beta_1, z). \\ W &= a_2^{2\beta_1 - 2} e^z z^{\beta_1 - 2} \sin(\pi\beta_1)/\pi. \end{aligned} \quad (53)$$

However, in the vicinity of infinity the numerically satisfactory pair is, Olver (1997)

$$\begin{aligned} y_1(\chi) &= (a_2 z)^{\beta_1 - 1} U(\alpha_1, \beta_1, z), \\ y_2(\chi) &= e^z (a_2 z)^{\beta_1 - 1} U(\beta_1 - \alpha_1, \beta_1, -z). \\ W &= (-1)^{\alpha_1 - \beta_1} a_2^{2\beta_1 - 2} e^z z^{\beta_1 - 2}. \end{aligned} \quad (54)$$

4.2. Local variance piecewise linear in the strike space

Another tractable model is where the local variance is piecewise linear in the strike space. In particular, this is the model we used in Carr and Itkin (2018).

⁴Due to the linearity of the degenerate Hypergeometric equation any linear combination of Kummer's functions also solves this equation.

Similar to the previous section, the corresponding continuous piecewise linear local variance function $v_j(x)$ at the interval $[x_i, x_{i+1}]$ reads

$$v_{j,i}(x) = v_{j,i}^0 + v_{j,i}^1 x, \quad (55)$$

where, however, it is now a function of x rather than χ . Since $v_j(x)$ is a continuous function in x , we have

$$v_{j,i}^0 + v_{j,i}^1 x_{i+1} = v_{j,i+1}^0 + v_{j,i+1}^1 x_{i+1}, \quad i = 0, \dots, n_j - 1. \quad (56)$$

This means that the first derivative of $v_j(x)$ experiences a jump at points x_i , $i \in Z \cap [1, n_j]$. As we assumed that $v(x, T)$ is a piecewise constant function of time, $v_{j,i}^0, v_{j,i}^1$ don't depend on T at the intervals $[T_j, T_{j+1}]$, $j \in 0, M - 1$, and jump to the new values at the points T_j , $j \in Z \cap [1, M]$.

The Eq.(46) can be solved by induction. One starts with $T_0 = 0$, and at each time interval $[T_{j-1}, T_j]$, $j \in Z \cap [1, M]$ solves the problem Eq.(46) for $V(x)$, and then obtains $P(S, T_j, x)$ from Eq.(45). Accordingly, the solution of Eq.(46) can be constructed separately for each interval $[x_{i-1}, x_i]$.

Substituting the representation Eq.(55) into Eq.(46), for the i -th spatial interval we obtain

$$\begin{aligned} -(b_2 + a_2 x)x^2 V_{x,x}(x) + b_1 x V_x(x) + b_{0,j} V(x) &= c(x), \\ b_2 &= v_{j,i}^0, \quad a_2 = v_{j,i}^1. \end{aligned} \quad (57)$$

Again, Eq.(57) is an *inhomogeneous* ordinary differential equation, and its solution can be represented in the form of Eq.(51) with

$$I_{12}(x) = -y_2(x) \int \frac{y_1(x)c(x)}{(b_2 + a_2 x)x^2 W(x)} dx + y_1(x) \int \frac{y_2(x)c(x)}{(b_2 + a_2 x)x^2 W(x)} dx \equiv J_1 + J_2. \quad (58)$$

The corresponding homogeneous equation can be solved as follows. First, if $b_2 \neq 0$ we make a change of independent variable $x \mapsto z = -a_2 x/b_2$. As the result the homogeneous Eq.(57) takes the form

$$b_2(z-1)zV_{z,z}(z) + b_1zV_z(z) + b_0V(z) = 0. \quad (59)$$

Then we make a change of the dependent variable $V(z) \mapsto z^m G(z)$ with m being some constant for the given time slice. This leads to the equation

$$\begin{aligned} z^m[\gamma + b_2(m-1)mz]G(z) + z^{m+1}[b_1 + 2b_2m(z-1)]G'(z) + b_2(z-1)z^{m+2}G''(z) &= 0, \\ \gamma &= b_0 + m(b_2 + b_1 - b_2m). \end{aligned} \quad (60)$$

Next we solve for m which makes γ vanishing, to obtain

$$m^\pm = \frac{b_2 + b_1 \pm \sqrt{4b_2b_0 + (b_2 + b_1)^2}}{2b_2}. \quad (61)$$

It is worth mentioning that if the determinant D in this expression is negative, both m^+ , m^- become complex. However, this is not a problem for the solution as coefficients C_1, C_2 in Eq.(51) could be complex as well, and such that the Put price is real.

Substituting this into Eq.(60) and rearranging we obtain

$$-m(m-1)G(z) + \left(2m - \frac{b_1}{b_2} - 2mz\right)G'(z) + z(1-z)G''(z) = 0, \quad m \in [m^+, m^-], \quad (62)$$

which is a Hypergeometric equation. As m can take two values, we need to choose the right one such that the final solution would obey the boundary conditions.

Combining all the above steps together, the solution of Eq.(59) could be written as

$$\begin{aligned} y_1(x) &= z^m [{}_2F_1(m-1, m, c; z)], \\ y_2(x) &= z^m [z^{1-c} {}_2F_1(m-c, m+1-c, 2-c; z)], \\ m &= m^+, \quad c = 2m - \frac{b_1}{b_2}, \quad z = -\frac{a_2}{b_2}x, \end{aligned} \quad (63)$$

Here ${}_2F_1(a, b, c; z)$ is the ordinary Hypergeometric function, Olver (1997). It has regular singularities at $z = 0, 1, \infty$. In terms of the solution in Eq.(52), these singularities correspond to $K = 0$, $v = 0$ and $K \rightarrow \infty$. We will show below that at $K \rightarrow \infty$ the coefficient a_2 for this interval is usually positive, so the variance is positive. However, the sign of b_2 could be both plus and minus. Therefore, if $b_2 > 0$ at this interval, we have $x \rightarrow \infty$, $z \rightarrow -\infty$. If $b_2 < 0$ at this interval, we have $x \rightarrow \infty$, $z \rightarrow \infty$.

When none of $c, c-a-b, a-b$ is an integer, we have a pair of fundamental solutions $f_1(x), f_2(x)$ that in Eq.(52) are represented by expressions in square brackets. It is known that this pair is numerically satisfactory, Olver (1997) aside of singularities at $z = 1$ and $z \rightarrow \infty$. Wronskian of these fundamental solutions $W(f_1(x), f_2(x))$ is

$$W(f_1(x), f_2(x)) = (1-c)z^{-c}(1-z)^{c-2m}, \quad z = -a_2x/b_2.$$

Accordingly,

$$W(y_1(x), y_2(x)) = -\frac{a_2(1-c)}{b_2}z^{2m-c}(1-z)^{c-2m}, \quad z = -a_2x/b_2. \quad (64)$$

In the vicinity of **singularity at $z = 1$** this pair, however, is not numerically satisfactory. Then we have to use another solution of Eq.(62) which is, Olver (1997)

$$\begin{aligned} y_1(x) &= z^m [{}_2F_1(m-1, m, 2m-c; 1-z)], \\ y_2(x) &= z^m [(1-z)^{c-2m+1} {}_2F_1(c-m+1, c-m, c-2m+2; 1-z)], \\ W(y_1(x), y_2(x)) &= -\frac{a_2(2m-1-c)}{b_2}(1-z)^{c-2m}z^{2m-c}, \quad z = -a_2x/b_2. \end{aligned} \quad (65)$$

The numerically satisfactory fundamental solutions in the vicinity of **singularity at $z = \infty$** is described in Appendix A.

However, we cannot use this solution at $z \rightarrow \infty$ as well as to use the solution in Eq.(63) at $z \rightarrow 0$. This is caused by the Roger Lee's moment matching formula, Lee (2004) which states that in the wings the implied variance surface should be at most linear in the normalized strike (or log-strike). It is also shown in De Marco et al. (2013); Gerhold and Friz (2015), that the asymptotic behavior of the local variance is linear in the log strike at both $K \rightarrow \infty$ and $K \rightarrow 0$. While the result for $K \rightarrow 0$ is shown to be true at least for the Heston and Stein-Stein models, the result for $K \rightarrow \infty$ directly follows from Lee's moment formula for the implied variance v_I and the representation of σ^2 via the total implied variance $w = v_I T$, Lipton (2001); Gatheral (2006)

$$w_L \equiv \sigma^2(T, K)T = \frac{T \partial_T w}{\left(1 - \frac{X \partial_X w}{2w}\right)^2 - \frac{(\partial_X w)^2}{4} \left(\frac{1}{w} + \frac{1}{4}\right) + \frac{\partial_X^2 w}{2}}, \quad (66)$$

where $w = w(X, T)$, $X = \log K/F$ and $F = S e^{(r-q)T}$ is the stock forward price.

Thus, the considered model of the local variance linear in strike is not applicable at the first $0 \leq x \leq x_1$ and the last $x_{n_j} < x < \infty$ strike intervals for every smile $T = T_j$ as it violets Lee's formula. Therefore, at these two intervals we use the model discussed in Section 4.1 where the local variance is linear in the log-strike.

It is interesting to mention, that in Itkin and Lipton (2018); Carr and Itkin (2018) and in section 4.1 the closed form solution was obtained in terms of Kummer's functions. Here the solution is expressed via Hypergeometric functions ${}_2F_1(a, b, c; x)$.

As two solutions $y_1(x)$ and $y_2(x)$ are independent, Eq.(51) is a general solution of Eq.(57). Two constants C_1, C_2 should be determined based on the boundary conditions for the function $y(x)$.

The boundary conditions for the ODE Eq.(57) in the x space at zero and infinity are given in Eq.(47), i.e. they are homogeneous. Based on the usual shape of the local variance curve and its positivity, for $x \rightarrow 0$, we expect that $v_{j,i}^1 < 0$. Similarly, for $x \rightarrow \infty$ we expect that $v_{j,i}^1 > 0$. In between these two limits the local variance curve for a given maturity T_j is assumed to be continuous, but the slope of the curve could be both positive and negative, see, e.g., Itkin (2015) and references therein.

4.3. Local volatility piecewise linear in the strike space

Another popular model is where the local volatility is assumed to be piecewise linear in the strike space. This model previously was frequently considered in the literature, e.g., Hull and White (2015); Kienitz and Caspers (2017). Below we show that with this assumption our model remains tractable, and a closed form solution can be obtained by using the same approach as elaborated on in Itkin and Lipton (2018); Carr and Itkin (2018).

Accordingly, the corresponding continuous piecewise linear local volatility function $\sigma_j(x)$ on the interval $[x_i, x_{i+1}]$ reads

$$\sigma_{j,i}(x) = \sigma_{j,i}^0 + \sigma_{j,i}^1 x, \quad (67)$$

Since $\sigma_j(x)$ is a continuous function in x , we have

$$\sigma_{j,i}^0 + \sigma_{j,i}^1 x_{i+1} = \sigma_{j,i+1}^0 + \sigma_{j,i+1}^1 x_{i+1}, \quad i = 0, \dots, n_j - 1. \quad (68)$$

Again, this means that the first derivative of $\sigma_j(x)$ experiences a jump at points x_i , $i \in Z \cap [1, n_j]$. As $\sigma(x, T)$ is a piecewise constant function of time, $\sigma_{j,i}^0, \sigma_{j,i}^1$ do not depend on T at the intervals $[T_j, T_{j+1})$, $j \in 0, M - 1$, and jump to the new values at the points T_j , $j \in Z \cap [1, M]$.

Substituting the representation Eq.(67) into Eq.(46), for the i -th spatial interval we obtain

$$-(b_2 + a_2 x)^2 x^2 V_{x,x}(x) + b_1 x V_x(x) + b_0 V(x) = c(x), \quad (69)$$

$$b_2 = \sigma_{j,i}^0, \quad a_2 = \sigma_{j,i}^1.$$

Again, Eq.(69) is an *inhomogeneous* ordinary differential equation, and its solution can be represented in the form of Eq.(51) with

$$I_{12}(x) = -y_2(x) \int \frac{y_1(x)c(x)}{(b_2 + a_2 x)^2 x^2 W(x)} dx + y_1(x) \int \frac{y_2(x)c(x)}{(b_2 + a_2 x)^2 x^2 W(x)} dx \equiv L_1 + L_2.$$

The corresponding homogeneous equation can be solved as follows. First, if $b_2 \neq 0, b_2 + a_2 x \neq 0$ we make a change of independent variable $x \mapsto z = a_2 b_1 x / [b_2^2 (b_2 + a_2 x)]$. As the result the homogeneous Eq.(69) takes the form

$$b_2 z^2 (-b_1 + b_2^2 z) V_{z,z}(z) + z [2b_2^4 z + (b_1 - b_2^2 z)^2] V_z(z) + b_0 (b_1 - b_2^2 z) V(z) = 0.$$

Next we make a change of the dependent variable

$$V(z) \mapsto z^{k_1} \left(\frac{z}{b_2^2 z + b_1} \right)^{k_2} G(z)$$

with k_1, k_2 being some constants for the given time slice. This leads to the equation

$$0 = -b_2^2 z (b_1 - b_2^2 z)^2 G''(z) + f_1(z) G'(z) + f_0(z) G(z), \quad (70)$$

$$f_1(z) = z (b_1 - b_2^2 z) [b_2^4 z (2k_1 + z + 2) - 2b_2^2 b_1 (k_1 + k_2 + z) + b_1^2],$$

$$f_0(z) = q_0 + q_1 z + q_2 z^2 - b_2^6 k_1 z^3,$$

$$q_2 = b_2^4 [b_0 - b_2^2 k_1 (k_1 + 1) + b_1 (3k_1 + k_2)],$$

$$q_1 = b_2^2 b_1 [2b_2^2 k_1 (k_1 + k_2) - 2b_0 - b_1 (3k_1 + 2k_2)],$$

$$q_0 = b_1^2 [b_0 - (k_1 + k_2) (b_2^2 (k_1 + k_2 - 1) - b_1)].$$

We now request that $f_0(z)$ is proportional to $z (b_1 - b_2^2 z)^2$ with some constant multiplier q , i.e.

$$f_0(z) = qz (b_1 - b_2^2 z)^2.$$

Solving this equation term by term in powers of z , we obtain

$$k_1 = -\frac{q}{b_2^2}, \quad k_2 = \frac{q(b_1 + q) - b_2^2(b_0 + q)}{b_2^2 b_1}, \quad q = \frac{1}{2} \left(b_2^2 - b_1 \pm \sqrt{b_2^4 + 2b_2^2(2b_0 + b_1) + b_1^2} \right).$$

Accordingly, substituting these definitions into Eq.(70) one finds

$$0 = zG''(z) + (b + z)G'(z) - aG(z),$$

$$b = 2 - \frac{b_1 + 2q}{b_2^2}, \quad a = \frac{q}{b_2^2}.$$

This is a sort of Kummer equation which has two independent solutions, Polyanin and Zaitsev (2003)

$$G(z) = e^{-z}U(a + b, b, z), \quad G(z) = e^{-z}M(a + b, b, z). \quad (71)$$

Accordingly, as q can take two values corresponding to the plus and minus sign, we have four fundamental solutions of the original equation Eq.(70).

Similar to the previous section, we cannot use these solutions at the first $0 \leq x \leq x_1$ and the last $x_{n_j} < x < \infty$ strike intervals for every smile $T = T_j$ as it violets Lee's formula. Therefore, at these two intervals we use the model discussed in Section 4.1 where the local variance is linear in the log-strike. Accordingly, the local volatility is a square root of the local variance.

5. Computation of the source term

Computation of the source term pI_{12} in Eq.(51) could be achieved in several ways. The most straightforward one is to use numerical integration since the Put price $P(x, T_{i-1})$ as a function of x is already known when we solve Eq.(51) for $T = T_i$. We underline that this is not the case in Itkin and Lipton (2018), because there the function $P(x, T_{i-1})$ is obtained by using an inverse Laplace transform, and as such is known only for a discrete set of strikes at the previous time level. Therefore, some kind of interpolation is necessary to find the local variance at all strikes when doing integration. Moreover, this interpolation must preserve no-arbitrage, see Itkin and Lipton (2018).

On the other hand, using no-arbitrage interpolation provides another advantage, as it makes it possible to compute the source term integrals in closed form if the interpolating function is wisely chosen. Here we want to exploit the same idea, thus significantly improving computational performance of our model as compared with the numerical integration.

Below as an example consider the case of the local variance piecewise linear in the strike space. Then based on solutions found in Section 4.2 in Eq.(63) we have

$$J_1(x) = -y_2(x) \int \frac{y_1(x)c(x)}{(b_2 + a_2x)x^2W(x)} dx = -y_2(x) \frac{a_2^2}{b_2^3} \int \frac{y_1(z)c(z)}{(1-z)z^2W(z)} dz, \quad (72)$$

$$y_1(z) = z^m {}_2F_1(m-1, m, c; z), \quad c(z) = V(S, T_{j-1}, z), \quad z = -a_2x/b_2,$$

where $W(z)$ is defined in Eq.(64).

Following the idea of Itkin and Lipton (2018), in Carr and Itkin (2018)) we introduced a non-linear interpolation

$$\begin{aligned} P(x) &= \gamma_0 + \gamma_2 x^2, \quad x_1 \leq x \leq x_3, \\ \gamma_0 &= \frac{P(x_3)x_1^2 - P(x_1)x_3^2}{x_1^2 - x_3^2}, \quad \gamma_2 = \frac{P(x_1) - P(x_3)}{x_1^2 - x_3^2}. \end{aligned} \quad (73)$$

Then Proposition 6.1 in Carr and Itkin (2018)) proves that this interpolation scheme is arbitrage-free.

It is worth emphasizing that the proposed interpolation doesn't affect the solution values (quotes) at given market strikes since the piecewise interpolator is constructed to exactly match those values. So the interpolation only affects the Put values that are not known, i.e., those with strikes that lie in between the given market strikes. Therefore, if these strikes are not used, i.e. in trading or hedging, the influence of the interpolation is unobservable at all. If, however, they are used for some purpose, the difference with the exact solution is small (within the error of interpolation), while the approximate solution for these strikes yet preserves no-arbitrage.

Recall, that we introduced $V(x)$ using Eq.(45). Accordingly, the term $c(z)$ in Eq.(72) takes the form (see Appendix D and Eq.(D.3))

$$c(z) = V(S, T_{j-1}, z) = \bar{\gamma}_0 + \gamma_1 z + \bar{\gamma}_2 z^2. \quad (74)$$

It turns out that now the integral in Eq.(72) can be computed in closed form. Indeed

$$\begin{aligned} \int \frac{y_1(z)c(z)}{(1-z)z^2W(z)} dz &= I_0 + I_1 + I_2, \\ I_0 &= \gamma_0 \int \frac{y_1(z)}{(1-z)z^2W(z)} dz = \bar{\gamma}_0 A(z) \frac{1}{\Gamma(c)(c-m-1)} {}_2F_1(c-m-1, c-m+1, c, z), \\ I_1 &= \gamma_1 \int \frac{zy_1(z)}{(1-z)z^2W(z)} dz = \gamma_1 z A(z) \frac{1}{\Gamma(c)(c-m)} {}_2F_1(c-m, c-m, c, z) \\ I_2 &= \bar{\gamma}_2 \int \frac{z^2 y_1(z)}{(1-z)z^2W(z)} dz = \bar{\gamma}_2 A(z) z^2 \frac{1}{(c-m+1)\Gamma(c)} {}_3F_2 \left[\begin{matrix} c-m, c-m+1, c-m+1 \\ c, 2+c-m \end{matrix}; z \right], \\ A(z) &= \frac{b_2}{a_2} \Gamma(c-1) z^{c-m-1}, \end{aligned} \quad (75)$$

where ${}_3F_2 \left[\begin{matrix} a_1, a_2, a_3 \\ b_1, b_2 \end{matrix}; z \right]$ is a generalized Hypergeometric function (Askey and Daalhuis (2010)).

The second integral in the definition of J_2

$$\begin{aligned} J_2(x) &= y_1(x) \int \frac{y_2(x)c(x)}{(b_2 + a_2 x)x^2W(x)} dx = y_1(x) \frac{a_2^2}{b_2^2} \int \frac{y_2(z)c(z)}{(1-z)z^2W(z)} dz, \\ y_2(z) &= z^{m+1-c} {}_2F_1(m-c, m+1-c, 2-c; z), \end{aligned} \quad (76)$$

could be computed in a similar way. The result reads

$$\begin{aligned}
\int \frac{y_2(z)c(z)}{(1-z)z^2W(z)}dz &= \mathcal{I}_0 + \mathcal{I}_1 + \mathcal{I}_2, \tag{77} \\
\mathcal{I}_0 &= \gamma_0 \int \frac{y_2(z)}{(1-z)z^2W(z)}dz = \bar{\gamma}_0 A(z) \frac{1}{m} {}_2F_1(2-m, -m, 2-c, z), \\
\mathcal{I}_1 &= \gamma_1 \int \frac{zy_2(z)}{(1-z)z^2W(z)}dz = \gamma_1 A(z) z \frac{1}{(m-1)} {}_2F_1(1-m, 1-m, 2-c, z), \\
\mathcal{I}_2 &= \bar{\gamma}_2 \int \frac{z^2y_2(z)}{(1-z)z^2W(z)}dz = \bar{\gamma}_2 A(z) z^2 \frac{1}{(m-2)} {}_3F_2 \left[\begin{matrix} 1-m, 2-m, 2-m \\ 2-c, 3-m \end{matrix}; z \right], \\
A(z) &= \frac{b_2}{a_2} \frac{\Gamma(1-c)}{\Gamma(2-c)} z^{-m},
\end{aligned}$$

Two special cases are the first $0 \leq x \leq x_1$ and the last $x_{n_j} < x < \infty$ intervals where the solution is given by Eq.(53) and Eq.(54).

5.1. Last interval $x_{n_j} \leq x < \infty$.

Since the right edge of this interval lies at infinity, the interpolation scheme in Eq.(73) should be slightly modified. This could be done twofold. The first option is to move the boundary from infinity to any very large but finite positive strike. Then the scheme in Eq.(73) could be used with no problem. But in our case it turns out that we are not able to compute these integrals in closed form. Therefore, we use another option which consists in replacing the quadratic form in Eq.(73) with another nonlinear interpolation

$$c(\chi) = V(\chi, T_{j-1}, S) = \gamma_\infty z^{-\nu}, \quad z = \chi + \frac{b_2}{a_2}, \tag{78}$$

where $\gamma_\infty > 0$, $\nu > 0$ are some constants to be determined. Obviously, at $\chi \rightarrow \infty$ this interpolation preserves the correct boundary value of V as in Eq.(47), i.e. $V(\chi)$ vanishes in this limit. Derivation of the appropriate values of γ_∞ , ν and a proof that the proposed interpolation preserves no-arbitrage are given in Appendix B.

Recall that at this interval we assume the local variance to be linear in the log-strike χ . Therefore, the numerically stable pair of solutions of Eq.(51) is given in Eq.(54). Then the integral in Eq.(51) can be computed in closed form. In doing so we use the following notation from Ng and Geller (1970)

$$\begin{aligned}
\int e^{-\alpha z} z^\nu U(a, b, z) dz &= U_\nu(\alpha; a, b, z), \\
\int e^{-\alpha z} z^\nu M(a, b, z) dz &= M_\nu(\alpha; a, b, z).
\end{aligned}$$

Then

$$\begin{aligned}
I_{12}(\chi) &= y_2(\chi) \int \frac{y_1(\chi)c(\chi)}{(b_2 + a_2\chi)W} d\chi - y_1(\chi) \int \frac{y_2(\chi)c(\chi)}{(b_2 + a_2\chi)W} d\chi, \\
\int \frac{y_1(\chi)c(\chi)}{(b_2 + a_2\chi)W} d\chi &= \xi_\infty \int e^{-z} z^{-\nu} U(\alpha_1, \beta_1, z) dz = \xi_\infty U_{-\nu}(-1; \alpha_1, \beta_1, z), \\
\int \frac{y_2(\chi)c(\chi)}{(b_2 + a_2\chi)W} d\chi &= \xi_\infty \int z^{-\nu} U(\beta_1 - \alpha_1, \beta_1, -z) dz = (-1)^{-\nu} \xi_\infty U_{-\nu}(0; \beta_1 - \alpha_1, \beta_1, -z), \\
\xi_\infty &= (-1)^{\beta_1 - \alpha_1} \gamma_\infty a_2^{2 - \beta_1}.
\end{aligned} \tag{79}$$

As per Ng and Geller (1970),

$$\begin{aligned}
M_\nu(-1; a, b, z) &= e^{i\pi(\nu+1)} M_\nu(0; b - a, b, -z), \\
M_\nu(0; a, b, z) &= \frac{z^{\nu+1}}{\nu+1} {}_2F_2 \left[\begin{matrix} \nu+1, a \\ \nu+2, b \end{matrix} ; z \right], \quad b \neq 0, -1, -2, \dots, \quad \nu \neq -1, -2, \dots, \\
M_{-1}(0; a, b, z) &= \frac{a}{b} z {}_3F_3 \left[\begin{matrix} a+1, 1, 1 \\ b+1, 2, 3 \end{matrix} ; z \right] + \log(z), \\
U_\nu(\alpha; a, b, z) &= \frac{\pi}{\sin(\pi b)} \left[\frac{M_\nu(\alpha; a, b, z)}{\Gamma(1+a-b)\Gamma(b)} - \frac{M_{\nu+1-b}(\alpha; 1+a-b, 2-b, z)}{\Gamma(a)\Gamma(2-b)} \right].
\end{aligned} \tag{80}$$

Therefore, all necessary integrals could be expressed in terms of generalized Hypergeometric functions. Alternatively, these integrals could be represented as

$$\begin{aligned}
U_{-\nu}(-1; \alpha_1, \beta_1, z) &= G_{2,3}^{2,1} \left(\begin{matrix} 1, 2+\alpha_1-\beta_1-\nu \\ 1-\nu, 2-\beta_1-\nu, 0 \end{matrix} \middle| z \right), \\
U_{-\nu}(0; \alpha_1, \beta_1, -z) &= \frac{z^{1-\nu}}{\Gamma(1-\alpha_1)\Gamma(\beta_1-\alpha_1)} G_{2,3}^{2,2} \left(\begin{matrix} \nu, 1+\alpha_1-\beta_1 \\ 0, 1-\beta_1, \nu-1 \end{matrix} \middle| -z \right),
\end{aligned} \tag{81}$$

where $G_{p,q}^{m,n} \left(\begin{matrix} a_1, \dots, a_p \\ b_1, \dots, b_q \end{matrix} \middle| z \right)$ is the Meijer G-function, see Olver (1997).

It is not difficult to verify that at $K \rightarrow \infty$, and so $z \rightarrow \infty$, the integral $I_{12}(\chi)$ vanishes.

5.2. First interval $0 \leq x \leq x_1$.

Recall that at this interval we assume the local variance to be linear in the log-strike χ . Since at $K \rightarrow 0$ we have $\chi \rightarrow -\infty$, the numerically stable pair of solutions of Eq.(51) is still given by Eq.(54).

However, at this interval we need another interpolation scheme because the previously described schemes don't give rise to tractable integrals. However, this could be achieved by using, e.g., the following nonlinear interpolation

$$c(\chi) = V(\chi, T_{j-1}, S) = \omega_0 e^z / z, \quad z = \chi + \frac{b_2}{a_2}, \tag{82}$$

where $\omega_0 < 0$ is a constant to be determined. Obviously, at $K \rightarrow 0$, and so $z \rightarrow -\infty$, this interpolation preserves the correct boundary value of V as in Eq.(47), i.e. $V(\chi)$ vanishes in this limit. Derivation of the appropriate value of ω_0 and a proof that the proposed interpolation preserves no-arbitrage are given in Appendix C.

Now the integral in Eq.(51) can be computed in closed form

$$\begin{aligned}
I_{12}(\chi) &= y_2(\chi) \int \frac{y_1(\chi)c(\chi)}{(b_2 + a_2\chi)W} d\chi - y_1(\chi) \int \frac{y_2(\chi)c(\chi)}{(b_2 + a_2\chi)W} d\chi, \quad (83) \\
\int \frac{y_1(\chi)c(\chi)}{(b_2 + a_2\chi)W} d\chi &= \xi_0 \int z^{-1} U(\alpha_1, \beta_1, z) dz = \xi_0 U_{-1}(0; \alpha_1, \beta_1, z), \\
\int \frac{y_2(\chi)c(\chi)}{(b_2 + a_2\chi)W} d\chi &= \xi_0 \int e^z z^{-1} U(\beta_1 - \alpha_1, \beta_1, -z) dz = -\xi_0 U_{-1}(-1; \beta_1 - \alpha_1, \beta_1, z), \\
\xi_0 &= (-1)^{\beta_1 - \alpha_1} \omega_0 a_2^{-\beta_1}.
\end{aligned}$$

Representation of functions $U_{-1}(-1; \beta_1 - \alpha_1, \beta_1, z)$, $U_{-1}(0; \alpha_1, \beta_1, z)$ via the Meijer G-function is given in Eq.(81). Again, it can be easily verified that at $K \rightarrow 0$, and so $z \rightarrow -\infty$, the integral $I_{12}(\chi)$ vanishes.

5.3. Special case $z \approx 1$ or $|v/b_2| \ll 1$.

This case occurs when at the interval $[K_i, K_{i+1}]$ for some $i \in [1, n_j]$ coefficients a_2, b_2 are such that either $|1 - z_i| \ll 1$ or $|1 - z_{i+1}| \ll 1$. Suppose, e.g. that $z_{i+1} = 1 + \epsilon$ with $0 < \epsilon \ll 1$. As shown in the next section, then we can introduce a ghost point K_* such that $z_* = 1 - \epsilon$. So at the interval $[K_*, K_{i+1}]$ we will use the numerically stable solution in Eq.(65), while at the interval $[K_i, K_*]$ - the regular solution in Eq.(63). Same construction could be provided if $z_i = 1 - \epsilon$.

At the interval $z \in [1 - \epsilon, 1 + \epsilon]$ where the values of z are close to singularity of the Hypergeometric function at $z = 1$ there are two ways to construct the solution. First, one can build an asymptotic solution using v/b_2 as a small parameter, because at $z \rightarrow 1$ we have $v/b_2 = (b_2 + a_2x)/b_2 = 1 - z \rightarrow 0$. As shown in Carr and Itkin (2018), this can be done, e.g., using the method of boundary functions, Vasil'eva et al. (1995).

Alternatively, it follows from Eq.(65) that $y_1(z) \rightarrow 1$, $y_2(z) \rightarrow 0$ at $z \rightarrow 1$. Therefore, these solutions have a regular behavior in the vicinity of $z = 1$. So all we need to do is to propose a suitable no-arbitrage interpolation to make computation of the source term in Eq.(58) tractable. This interpolation is constructed in Appendix D.

Thus, based on Eq.(72) and Eq.(65) we need to compute 2 integrals

$$\begin{aligned}
\mathcal{J}_1(x) &= \int \frac{y_1(z)c(z)}{(1-z)z^2W(z)} dz, & \mathcal{J}_2(x) &= \int \frac{y_2(z)c(z)}{(1-z)z^2W(z)} dz, \quad (84) \\
y_1(z) &= z^m {}_2F_1(m-1, m, 2m-c; 1-z), & c(z) &= V(z, T_{j-1}, S), \\
y_2(z) &= z^m (1-z)^{c-2m+1} {}_2F_1(c-m+1, c-m, c-2m+2; 1-z),
\end{aligned}$$

$$W(y_1(z), y_2(z)) = \omega_1(1-z)^{c-2m} z^{2m-c}, \quad \omega_1 = -\frac{a_2(2m-1-c)}{b_2}.$$

The integral $\mathcal{J}_2(x)$ can be found in closed form, and the result reads

$$\begin{aligned} \mathcal{J}_2(x) &= \bar{\gamma}_0 \mathcal{J}_{2,0}(x) + \gamma_1 \mathcal{J}_{2,1}(x) + \bar{\gamma}_2 \mathcal{J}_{2,1}(x), \tag{85} \\ \mathcal{J}_{2,0}(x) &= \frac{\pi}{\omega_1} \csc(\pi c) z^{-m} \Gamma(c-2m+2) \left[\frac{z^{c-1} {}_2F_1(c-m-1, c-m+1; c; z)}{(c-m-1)\Gamma(c)\Gamma(1-m)\Gamma(2-m)} \right. \\ &\quad \left. + \frac{{}_2F_1(2-m, -m; 2-c; z)}{m\Gamma(2-c)\Gamma(c-m)\Gamma(c-m+1)} \right], \\ \mathcal{J}_{2,1}(x) &= \frac{\pi}{(m-1)\omega_1} \csc(\pi c) z^{-m} \Gamma(c-2m+2) \left[\left(\frac{z^{c-m} {}_2F_1(1-m, 1-m; 2-c; z)}{\Gamma(2-c)\Gamma(c-m+1)^2} \right. \right. \\ &\quad \left. \left. - \frac{z^c {}_2F_1(c-m, c-m; c; z)}{(c-m)\Gamma(c)\Gamma(1-m)^2} \right) \right], \\ \mathcal{J}_{2,2}(x) &= \frac{\Gamma(c-2m+2)}{\omega_1 \Gamma(1-m)\Gamma(2-m)\Gamma(c-m)\Gamma(c-m+1)} G_{3,3}^{2,3} \left(\begin{matrix} 1, 1, 2 \\ 2-m, c-m+1, 0 \end{matrix} \middle| z \right). \end{aligned}$$

The integral $\mathcal{J}_1(x)$ with the use of no-arbitrage interpolation defined in Eq.(D.3) reads

$$\mathcal{J}_1(x) = \omega_1^{-1} \int (1-z)^{-c+2m-1} z^{c-m-2} {}_2F_1(m-1, m; 2m-c; 1-z) (\bar{\gamma}_0 + \gamma_1 z + \bar{\gamma}_2 z^2) dz.$$

This integral can be computed as follows. We remind that $z \in [1-\epsilon, 1+\epsilon]$, $|\epsilon| \ll 1$. Therefore, the term z^k , $k \in \mathbb{R}$ can be expanded into series around $z = 1$ to obtain

$$z^k = \sum_{i=0}^{\infty} (-1)^i \binom{k}{i} (1-z)^i$$

Then $\mathcal{J}_1(x)$ takes the form

$$\begin{aligned} \mathcal{J}_1(x) &= \omega_1^{-1} \left\{ \bar{\gamma}_0 \sum_{i=0}^{\infty} (-1)^i \binom{c-m-2}{i} \int (1-z)^{i-c+2m-1} {}_2F_1(m-1, m; 2m-c; 1-z) dz \right. \tag{86} \\ &\quad \left. + \gamma_1 \sum_{i=0}^{\infty} (-1)^i \binom{c-m-1}{i} \int (1-z)^{i-c+2m-1} {}_2F_1(m-1, m; 2m-c; 1-z) dz \right. \\ &\quad \left. + \bar{\gamma}_2 \sum_{i=0}^{\infty} (-1)^i \binom{c-m}{i} \int (1-z)^{i-c+2m-1} {}_2F_1(m-1, m; 2m-c; 1-z) dz \right\} \\ &= \omega_1^{-1} \sum_{i=0}^{\infty} \nu_i \int (1-z)^{i-c+2m-1} {}_2F_1(m-1, m; 2m-c; 1-z) dz, \end{aligned}$$

$$= \omega_1^{-1} \sum_{i=0}^{\infty} \frac{\nu_i}{c-i-2m} (1-z)^{-c+i+2m} {}_3F_2 \left[\begin{matrix} m-1, m, 2m-c+i \\ 2m-c, 2m+i-c+1 \end{matrix}; 1-z \right],$$

$$\nu_i = (-1)^i \left[\bar{\gamma}_0 \binom{c-m-2}{i} + \gamma_1 \binom{c-m-1}{i} + \bar{\gamma}_2 \binom{c-m}{i} \right].$$

The exponent $-c+i+2m = i + b_1/b_2$ is always positive if $b_2 > 0$ in the vicinity of $z = 1$. According to Appendix D, this condition on b_2 is valid if $1 - \epsilon \leq z < 1$. Therefore, 2-3 terms in the expansion Eq.(86) provide the sufficient accuracy in computation of the integral. However, this is also true when $1 + \epsilon > z > 1$ (and so b_2 is negative) which implies that the entire exponent is also negative, at least at low i . This is because the behavior of the product $(1-z)^{i-c+2m} {}_3F_2 \left[\begin{matrix} m-1, m, 2m-c+i \\ 2m-c, 2m+i-c+1 \end{matrix}; 1-z \right]$ is regular even in this case.

In a similar manner the source terms for other models of the local variance/volatility considered in previous sections could be computed in closed form. We leave this exercise to the reader.

6. Smile calibration for a single term.

Calibration problem for the local volatility model is described in Carr and Itkin (2018) as well as the construction of the solution for the entire smile. Here we follow the same approach, and, therefore, provide just some short comments specific to the GLVG model. Again, as an example consider the case where the local variance is a piecewise linear function of strike. Calibration for the other cases considered in Section 4 can be done in a similar manner.

A general calibration problem we need to solve is: given market quotes of Call and/or Put options corresponding to various strikes $\{K\} := K_j, j \in [1, N]$ and same maturity T_i , find the local variance function $v(x)$ such that these quotes solve equations in Eq.(37), Eq.(43).

Suppose that the Put prices for $T = T_j$ are known for n_j ordered strikes. The location of those strikes on the x line is schematically depicted in Fig. 1

Recall that the general form of the solution is given in Eq.(51) which at every interval $x_{i-1} \leq x \leq x_i$ and $T = T_j$ can be represented as

$$V(x) = C_{j,i}^{(1)} y_1(x) + C_{j,i}^{(2)} y_2(x) + I_{12}(x). \quad (87)$$

Here for better readability we changed the notation of two integration constants which belong to the i -th interval in x and j -th maturity to $C_{j,i}^{(1)}, C_{j,i}^{(2)}$.

Similar to Carr and Itkin (2018), we assume continuity of the options price and its first derivative at every node $i = 1, \dots, n_j$. We also supplement this by two additional conditions: the first one is given by Eq.(49), and the other one is that at every node the solution $P(S, T_j, K_i)$ must coincide with a given market quote for the pair (T_j, K_i) . So together this provides four equations

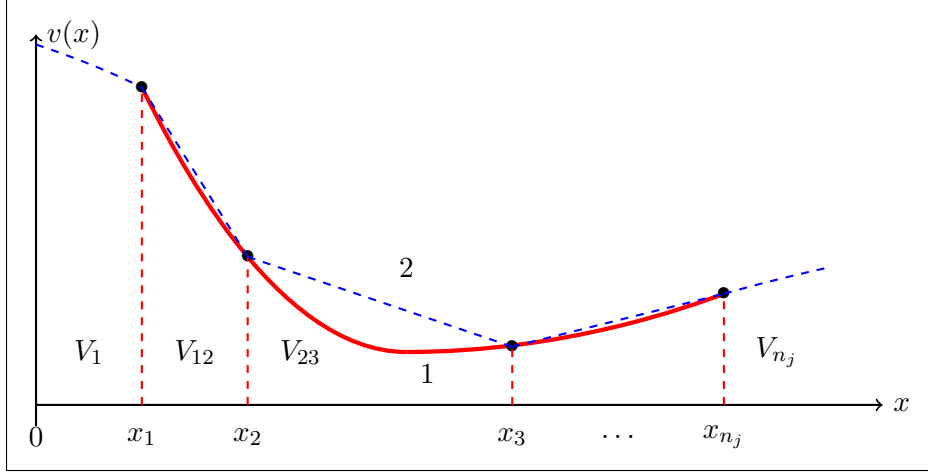


Figure 1: Schematic construction of the combined solution in $x \in \mathbb{R}^+$: 1 (red solid line) - the real (unknown) local variance curve, 2 (dashed blue line) - a piecewise linear solution. At $x > x_{n_j}$ and $x < x_1$ the blue line is $b_2 + a_2 \log(x)$.

for four unknown variables $v_{j,i}^0, v_{j,i}^1, C_{j,i}^{(1)}, C_{j,i}^{(2)}$:

$$\begin{aligned}
 P_i(x)|_{x=x_i} &= P_{i+1}(x)|_{x=x_i}, \\
 P_i(x)|_{x=x_i} &= P_{market}(x_i), \\
 \frac{\partial P_{i+1}(x)}{\partial x} \Big|_{x=x_i} &= \frac{\partial P_i(x)}{\partial x} \Big|_{x=x_i}, \\
 v_{j,i}^0 + v_{j,i}^1 x_i &= v_{j,i+1}^0 + v_{j,i+1}^1 x_i, \quad i = 1, \dots, n_j.
 \end{aligned} \tag{88}$$

The Eq.(88) is a system of $4n_j$ nonlinear equations with respect to $4(n_j + 1)$ variables $v_{j,i}^0, v_{j,i}^1, C_{j,i}^{(1)}, C_{j,i}^{(2)}$. Therefore we need 4 additional conditions to uniquely solve it.

To this end observe that the constants $C_{j,1}^{(2)}, C_{j,n_j}^{(2)}$ could be determined based on the boundary conditions in Eq.(47). Indeed, at $K \rightarrow 0$ function $y_2(\chi)$ in Eq.(54) vanishes (as $a_2 < 0$ at this interval), but not $y_1(x)$. Therefore, to obey the vanishing boundary condition in Eq.(47) we must set $C_{j,1}^{(1)} = 0$. As that was already discussed, the source term in Eq.(83) also vanishes in this limit. Therefore, the solution in Eq.(54) with the source term in Eq.(83) and $C_{j,1}^{(2)} = 0$ obeys the boundary condition at $z \rightarrow 0$.

At $K \rightarrow \infty$ based on representation of the solution in Eq.(54) with $a_2 > 0$ at this interval, similarly we must set $C_{j,n_j}^{(2)} = 0$, as the solution $y_2(x)$ in Eq.(54) diverges at $z \rightarrow \infty$.

The remaining two additional conditions could be set in many different ways. Here we rely on traders intuition about the asymptotic behavior of the volatility surface at strikes close to zero and infinity. According to our construction, they are determined by $v_{j,0}^1$ and v_{j,n_j}^1 . Therefore, we

assume these coefficients to be somehow known, i.e. consider them as the given parameters of our model.

Overall, by solving the nonlinear system of equations Eq.(88) we find the final solution of our problem. This can be done by using standard methods, and, thus, no any optimization procedure is necessary. However, a good initial guess still would be helpful for a better (and faster) convergence. Construction of such a guess is described in Carr and Itkin (2018). Also note that this system has a block-diagonal structure where each block is a 2x2 matrix. Therefore, it can be easily solved with the linear complexity $O(n_j)$.

When computing the first derivatives, we take into account that derivatives of Hypergeometric functions belong to the same class of functions, since, Abramowitz and Stegun (1964)

$$\begin{aligned}\frac{\partial}{\partial z} {}_2F_1(a, b, c, z) &= \frac{ab}{c} {}_2F_1(a+1, b+1, c+1, z), \\ \frac{\partial}{\partial z} {}_3F_2\left[\begin{matrix} a, b, c \\ d, e \end{matrix}; z\right] &= \frac{abe}{cd} {}_3F_2\left[\begin{matrix} a+1, b+1, c+1 \\ d+1, e+1 \end{matrix}; z\right].\end{aligned}$$

Same is true for the Meijer G-function. For instance,

$$\begin{aligned}\frac{\partial}{\partial z} G_{2,3}^{2,2}\left(\begin{matrix} \nu, 1+\alpha_1-\beta_1 \\ 0, 1-\beta_1, \nu-1 \end{matrix} \middle| -z\right) &= \frac{\Gamma(1-\alpha_1)\Gamma(\beta_1-\alpha_1)}{z} U(\beta_1-\alpha_1, \beta_1, -z) \\ &+ (\nu-1) G_{2,3}^{2,2}\left(\begin{matrix} \nu, 1+\alpha_1-\beta_1 \\ 0, 1-\beta_1, \nu-1 \end{matrix} \middle| -z\right).\end{aligned}\tag{89}$$

Therefore, computing derivatives of the solution does not cause any new technical problem.

6.1. Special case $|1 - z_i| \ll 1$ at some node K_i , $i \in [1, n_j]$.

Without loss of generality suppose that $z_i = 1 - \epsilon$ and $z_{i+1} \gg 1 + \epsilon$ with $0 < \epsilon \ll 1$. The other case $z_i = 1 + \epsilon$ and $z_{i-1} \ll 1 - \epsilon$ could be treated in a similar way. Then let us introduce a ghost point K_* such that $z_* = 1 + \epsilon$. So at the interval $[K_i, K_*]$ we will use the numerically stable solution in Eq.(65), while at the interval $[K_*, K_{i+1}]$ - the regular solution in Eq.(63).

Since K_* is the ghost point, we don't have a market quote available at K_* . All we can say is that yet we assume the local variance/volatility to be a piecewise linear function of K at $[K_*, K_{i+1}]$ and $[K_i, K_*]$. It has to be continuous but with a possible jump in skew at K_* .

Since a market quote at K_* is not available, we can replace it with any reasonable value. For instance, an interpolated value between market quotes at K_i, K_{i+1} could be used obtained by using

no-arbitrage interpolation⁵. Then we obtain four equations for $C_{j,*}^{(1)}, C_{j,*}^{(2)}, v_{j,*}^0, v_{j,*}^1$

$$\begin{aligned} P_i(x)|_{x=x_i} &= P_*(x)|_{x=x_i}, \\ P_*(x)|_{x=x_*} &= P_{interp}(x)|_{x=x_*}, \\ \frac{\partial P_*(x)}{\partial x} \Big|_{x=x_i} &= \frac{\partial P_i(x)}{\partial x} \Big|_{x=x_i}, \\ v_{j,i}^0 + v_{j,i}^1 x_* &= v_{j,*}^0 + v_{j,*}^1 x_*, \quad i = 1, \dots, n_j. \end{aligned} \tag{90}$$

that should be added to Eq.(88). Solving this new combined linear system in the same way as we did it for Eq.(88) we find the values of all unknown $C_{j,i}^{(1)}, C_{j,i}^{(2)}, v_{j,i}^0, v_{j,i}^1$ where now $i \in \{[1, n_j] \cup *\}$.

7. Discussion

First, let us mention that in many practical calculations either coefficients $a_2 = v_{j,i}^1$ at some i , or both $b_2 = v_{j,i}^0, a_2 = v_{j,i}^1$ (see, for instance, Eq.(57)) are small. Of course, in that case the general solution Eq.(63) remains valid. However, when computing the values of Hypergeometric functions numerically, the errors significantly grow in such a case. This is especially pronounced when computing the source term integral I_{12} . The main point is that either the Hypergeometric function takes a very small value, and then the constants $C_{j,i}^{(1)}, C_{j,i}^{(2)}$ should be very large to compensate, or vice versa. Resolution of this issue requires a high-precision arithmetics, and, which is more important, taking into account many terms in a series representation of the Hypergeometric functions, which significantly slows down the total performance of the method.

To eliminate these problems we can look at asymptotic solutions of Eq.(57) taking into account the existence of small parameters from the very beginning. This approach was successfully elaborated on in Itkin and Lipton (2018); Carr and Itkin (2018), so we don't describe it here in detail.

In Carr and Itkin (2018) we calibrated the ELVG model, e.g. to the data set taken from Balaraman (2016). In that paper an implied volatility surface of S&P500 is presented, and the local volatility surface is constructed using the Dupire formula. We took data for the first 12 maturities and all strikes as they are given in Balaraman (2016). Our results demonstrated high accuracy and speed of calibration.

When doing so, a technical note should be made. We mentioned already that in our model for every term the slopes of the smile at strikes close to zero, $v_{j,0}^1$ and infinity, v_{j,n_j}^1 are free parameters of the model. So often traders have an intuition about these values. However, in our numerical experiments we setup them just using some plausible test values. In particular, in Carr and Itkin (2018) for the sake of simplicity for all smiles we used $v_{j,0}^1 = -0.3$, and $v_{j,n_j}^1 = 0.1$. Accordingly, for

⁵Despite it looks attractive, we cannot require $v_{j,i}^1 = v_{j,*}^1$ since this also gives rise to $v_{j,i}^0 = v_{j,*}^0$. However, $v_{j,i}^0$ changes sign at $z = 1$.

the instantaneous variance $v_j(x_i) = p_j(v_{j,i}^0 + v_{j,i}^1 \log(x_i))/2$ the slopes at both zero and plus infinity are time-dependent and can be computed by using this definition.

As a numerical solver for the system of linear equations we used the standard Matlab *fsolve* function, and utilized a "trust-region-dogleg" algorithm. Parameter "TypicalX" has to be chosen carefully to speedup calculations.

In this paper we repeated this test, but now using the GLVG instead of the ELVG. The results look same as in Fig.5 of Carr and Itkin (2018), i.e. the quality of the fit is same, and performance of the method is almost same. But the conclusion of Carr and Itkin (2018) remains intact, namely that performance of this model is much better than that reported in both Itkin (2015) and Itkin and Lipton (2018).

Therefore, a natural question would be: which flavor of the Local Variance Gamma model - arithmetic or geometric one is preferable. Perhaps, if the ultimate goal is fast calibration of the given smile, both could be used interchangeably, and both are capable to provide a good and fast fit. However, for modeling option prices the difference between the geometric and arithmetic LVG models is of the same kind as between the Bachelier and Black-Scholes models. So, for instance, for modeling stock prices the latter would be preferable, while for modeling interest rates the former could provide negative values, which nowadays is a desirable feature.

8. Conclusions

In this paper we propose another flavor of the Local Variance Gamma. Several contributions are made as compared with the existing literature. First, the model is constructed based on a Gamma time-changed *geometric* Brownian motion with drift, while in all previous papers an arithmetic Brownian motion was used.

Second, we consider 2 models of the local variance - piecewise linear in strike, piecewise linear in the log-strike, and the model of the local volatility piecewise linear in strike (which is new in this context). We also consider a combined model of the local variance which is piecewise linear in strike in the internal intervals, and linear in the log-strike at the first and last intervals (see below in more detail).

Third, we show that for all these new constructions still it is possible to derive an ordinary differential equation for the option price, which plays a role of Dupire's equation for the standard local volatility model. Moreover, it can be solved in closed form in terms of various flavors of Hypergeometric functions. For doing so we propose several new versions of no-arbitrage interpolation, similar to how this was done in Carr and Itkin (2018) but in a slightly different form, so the entire approach becomes tractable.

Also we shortly discuss various asymptotic solutions which allow a significant acceleration of the numerical solver and improvement of its accuracy in that cases (i.e, when parameters of the model obey the conditions to apply the corresponding asymptotic). For the sake of brevity we omit the exact derivations as they can be obtained similar to how this is done in Carr and Itkin (2018).

Fourth, new boundary conditions are derived for the Put option in the GLVG. They are discrete and converge to the standard boundary conditions in the continuous case (Dupire). These conditions are constructed using some analog of discrete compounding which is natural for the LVG model.

And finally, we notice that for any piecewise model of the local variance/volatility at edge intervals where strikes are close either to 0 or to infinity one has to switch to the local variance linear in log-strike because of Roger Lee's moment formula. Thus, the whole local variance/volatility model becomes a combination of the original model at the internal intervals and local variance linear in log-strike at the edge intervals.

The other features of the GLVG model are pretty much inherited from the ELVG. For instance, similar to Carr and Itkin (2018), we show that given multiple smiles the whole local variance/volatility surface can be recovered that does not require solving any optimization problem. Instead, it can be done term-by-term by solving a system of non-linear algebraic equations for each maturity, which is faster.

Appendices

Appendix A. Numerically satisfactory solutions of Eq.(59) at $z \rightarrow \infty$.

According to Olver (1997), the numerically satisfactory fundamental solutions of Eq.(59) in the vicinity of **singularity at $z = \infty$** are

$$\begin{aligned} y_1(x) &= z^m [z^{-A} {}_2F_1(A, A - C + 1, A - B + 1, 1/z)], \\ y_2(x) &= z^m [z^{-B} {}_2F_1(B, B - C + 1, B - A + 1; 1/z)], \end{aligned} \tag{A.1}$$

where in our case $A = m - 1, B = m, C = c$. This substitution transforms the second solution in Eq.(A.1) to

$$y_2(x) = z^m [z^{-m} {}_2F_1(m, m - c + 1, 2; 1/z)], \tag{A.2}$$

and behaves well at $z \rightarrow \infty$. However, since in our setting $n \equiv A - B + 1 = m - 1 - m + 1 = 0$, and due to the property

$$\begin{aligned} \lim_{c \rightarrow -n} \frac{F(a, b, c; z)}{\Gamma(c)} &= \frac{(a)_{n+1} (b)_{n+1}}{(n+1)!} z^{n+1} F(a+n+1, b+n+1, n+2; z), \\ y_1(x) &= F(m-1, m-c, 0; z) = \Gamma(0) \frac{(m-1)_1 (m-c)_1}{(1)!} z F(m, m-c+1, 2; z), \end{aligned}$$

it turns out that the first solution differs from the second one just by a constant multiplier, i.e. they are not independent. Therefore, in this case instead the first solution $y_1(x)$ should

be chosen based on a more sophisticated analytic continuation of the Hypergeometric function, Bateman and Erdélyi (1953).

$$\begin{aligned}
y_1(x) &= z^m [(-z)^{1-m} \frac{\Gamma(c)}{\Gamma(m)\Gamma(c-m+1)} \Psi(z)], \quad |z| > 1, \quad |\text{ph}(-z)| < \pi, \quad (\text{A.3}) \\
\Psi(z) &= 1 - \frac{1}{z} \sum_{k=0}^{\infty} \frac{(m-1)_{k+1} (m-c)_{k+1}}{k!(k+1)!} z^{-k} [\log(-z) + \phi_k], \\
\phi_k &\equiv \psi(k+1) + \psi(k+2) - \psi(m+k) - \psi(c-m-k), \\
(m)_k &= \Gamma(m)/\Gamma(k), \quad \psi(x) = \Gamma'(x)/\Gamma(x).
\end{aligned}$$

Appendix B. No-arbitrage interpolation at $\chi \rightarrow \infty$.

In this Appendix we prove the following Proposition:

Proposition 1. *Recall that according to Eq.(78) the proposed interpolation scheme for $V(\chi, T_{j-1}, S)$ at the interval $x_{n_j} \leq x < \infty$ reads*

$$c(\chi) = V(\chi, T_{j-1}, S) = \gamma_{\infty} z^{-\nu}, \quad z = \chi + \frac{b_2}{a_2}, \quad (\text{B.1})$$

where $\gamma_{\infty} > 0$, $\nu > 0$ are some constants determined below in the proof. Also this scheme preserves no-arbitrage.

Proof By construction, at $K \rightarrow \infty$, $c(\chi)$ converges to the correct boundary condition, i.e. vanishes. Assuming that K_{n_j} is in-the-money, Eq.(78) can be re-written in the form

$$P(K) = A(T_{j-1})K - B(T_{j-1})S + \gamma_{\infty} [\log(K/S) + b_2/a_2]^{-\nu}. \quad (\text{B.2})$$

As at this interval $v = b_2 + a_2 \log(K/S) > 0$, and it was assumed that $K > S$, we must have $a_2 > 0$. Accordingly, to have a positive Put price we require $\gamma_{\infty} > 0$. This constant could be determined by using a known Put value at K_{n_j} , i.e. $P(K_{n_j}) = P_{n_j}$. This yields

$$\gamma_{\infty} = [P_{n_j} - A(T_{j-1})K_{n_j} - B(T_{j-1})S] \left[\frac{b_2}{a_2} + \log \left(\frac{K_{n_j}}{S} \right) \right]^{\nu} > 0. \quad (\text{B.3})$$

Therefore, this definition is also consistent with the requirement of positiveness of γ_{∞} .

As this is described in detail in Itkin and Lipton (2018), the no-arbitrage conditions for the Put price read

$$P > 0, \quad P_K > 0, \quad P_{K,K} > 0.$$

Differentiating Eq.(B.2) on K , and then again, we obtain

$$\begin{aligned} P'_K &= A(T_{j-1}) - \frac{\gamma_\infty \nu}{K} \left[\frac{b_2}{a_2} + \log \left(\frac{K}{S} \right) \right]^{-1-\nu}, \\ P''_K &= \frac{\gamma_\infty \nu}{a_2 K^2} \left[\frac{b_2}{a_2} + \log \left(\frac{K}{S} \right) \right]^{-\nu-2} [b_2 + a_2(1 + \nu + \log(K/S))]. \end{aligned} \quad (\text{B.4})$$

Analyzing these expressions we conclude that $P''_K > 0$. Observe that at $K \rightarrow \infty$ we also have $P'_K > 0$. Also observe that P'_K is a monotone function of K . Therefore, let us look at $P'_K(K_{n_j})$. Substitution of $K = K_{n_j}$ into the first line of Eq.(B.4) yields

$$P'_K(K_{n_j}) = A(T_{j-1}) + \frac{a_2 \nu}{K_{n_j}(b_2 + a_2 \log(K/S))} [A(T_{j-1})K_{n_j} - B(T_{j-1})S - P_{n_j}]. \quad (\text{B.5})$$

As the Put value exceeds its intrinsic value, $P'_K(K_{n_j})$ is positive if

$$0 < \nu < A(T_{j-1})K_{n_j} \left[\frac{b_2}{a_2} + \log \left(\frac{K_{n_j}}{S} \right) \right] [P_{n_j} - A(T_{j-1})K_{n_j} + B(T_{j-1})S]^{-1} \equiv \Omega. \quad (\text{B.6})$$

At large K_{n_j} the expression in the first square brackets is large, and in the second ones - small. Thus the upper boundary for ν is high enough.

Finally, we take into account the well-known upper bound of the Put option price which is, Hull (1997)

$$P_{n_j} \leq A(T_j)K_{n_j}.$$

Because of that, we can re-write Eq.(B.6) as

$$0 < \nu < \frac{A(T_{j-1})}{B(T_{j-1})} \frac{K_{n_j}}{S} \left[\frac{b_2}{a_2} + \log \left(\frac{K_{n_j}}{S} \right) \right] \approx \frac{K_{n_j}}{S} \left[\frac{b_2}{a_2} + \log \left(\frac{K_{n_j}}{S} \right) \right] \leq \Omega. \quad (\text{B.7})$$

Therefore, if ν is chosen according to Eq.(B.6) or Eq.(B.7), this guarantees that $P'_K(K_{n_j}) > 0$. As $P'_K(K)$ is a monotone function of K , this proves that with this choice of ν the condition $P'_K(K) > 0$ is valid at the whole interval $x_{n_j} \leq x < \infty$. Thus, this interpolation preserves no-arbitrage. ■

Appendix C. No-arbitrage interpolation at $\chi \rightarrow -\infty$.

In this Appendix we prove the following Proposition:

Proposition 2. *Recall that according to Eq.(78) the proposed interpolation scheme for $V(\chi, T_{j-1}, S)$ at the interval $-\infty \leq x < x_1$ reads*

$$V(\chi, T_{j-1}, S) = \omega_0 e^{z/z}, \quad z = \chi + \frac{b_2}{a_2}, \quad (\text{C.1})$$

where $\omega_0 = V(\chi_1, T_{j-1}, S) z_1 e^{-z_1} < 0$ is constant. Also this scheme preserves no-arbitrage.

Proof Obviously, at $K = K_1$ we have $\chi_1 = \log(K_1/S)$, $V(\chi, T_{j-1}, S) = V(\chi_1, T_{j-1}, S) \equiv V_1$, therefore, assuming the strike K_1 is out of the money

$$\omega_0 = V_1 z_1 e^{-z_1} < 0. \quad (\text{C.2})$$

As this is described in detail in Itkin and Lipton (2018), the no-arbitrage conditions for the Put price read

$$P > 0, \quad P_K > 0, \quad P_{K,K} > 0.$$

Based on Eq.(78) and the definition of V in Eq.(45), the Put price at this interval can be represented as

$$P(K, T_{j-1}, S) = \omega_0 e^z / z = \omega_0 e^{b_2/a_2} \frac{K/S}{\log(K/S) + b_2/a_2}. \quad (\text{C.3})$$

As at this interval $v = b_2 + a_2 \log(K/S)$, and it was assumed that $K < S$, we must have $a_2 < 0$. Accordingly, to have a positive Put price we require $\omega_0 < 0$. This is consistent with the value of ω_0 introduced in Eq.(C.2).

Differentiating Eq.(C.3) on K , and then again, we obtain

$$\begin{aligned} P'_K &= \frac{\omega_0 a_2}{S} e^{b_2/a_2} \frac{b_2 - a_2 + a_2 \log(K/S)}{(b_2 + a_2 \log(K/S))^2} > 0, \\ P''_K &= -\omega_0 \frac{a_2^2}{KS} e^{b_2/a_2} \frac{b_2 - 2a_2 + a_2 \log(K/S)}{(b_2 + a_2 \log(K/S))^3} > 0. \end{aligned} \quad (\text{C.4})$$

Thus, the proposed scheme can be used for interpolation because it provides correct Put option prices at $K = K_1$ and $K \rightarrow 0$, and is monotone in K . Moreover, it preserves no-arbitrage. \blacksquare

Appendix D. No-arbitrage interpolation at $z \rightarrow 1$.

As by definition in Eq.(63) $z = -\frac{a_2}{b_2}x$, this implies that

$$1 - z = 1 + \frac{a_2}{b_2}x = \frac{v_{ji}}{b_2}.$$

Obviously, $v_{ji} \geq 0$. Therefore, when z is close to 1 two situations are possible:

1. $z < 1$, which implies $b_2 > 0$, and accordingly $a_2 < 0$;
2. $z > 1$, which implies $b_2 < 0$, and accordingly $a_2 > 0$.

Suppose for interpolation of the Put price we use Eq.(73), i.e.

$$\begin{aligned} P(x) &= \gamma_0 + \gamma_2 x^2, \quad x_1 \leq x \leq x_3, \\ \gamma_0 &= \frac{P(x_3)x_1^2 - P(x_1)x_3^2}{x_1^2 - x_3^2} = P_1 - \frac{P_3 - P_1}{x_3^2 - x_1^2} x_1^2 > 0, \quad \gamma_2 = \frac{P(x_1) - P(x_3)}{x_1^2 - x_3^2} > 0. \end{aligned} \quad (\text{D.1})$$

The second inequality is obvious since $P(x_3) > P(x_1)$ if $x_3 > x_1$. The first one follows from the fact that the Put price exceeds its intrinsic value, i.e.

$$P_i = [A(T_j)K_i - B(T_j)S]^+ + \varepsilon_i, \quad \varepsilon_i > 0.$$

Suppose, e.g., that both strikes K_1, K_3 are in-the-money. Then

$$\begin{aligned} \gamma_0 &= P_1 - \frac{P_3 - P_1}{x_3^2 - x_1^2} x_1^2 = P_1 - \frac{A(T_j)S(x_3 - x_1) + \varepsilon_3 - \varepsilon_1}{x_3^2 - x_1^2} x_1^2 \\ &= \frac{P_1 x_3 + x_1(P_1 - A(T_j)K_1)}{x_3 + x_1} + \frac{\varepsilon_1 - \varepsilon_3}{x_3^2 - x_1^2} x_1^2 > 0, \end{aligned} \tag{D.2}$$

as based on the properties of the Put price $\varepsilon_1 > \varepsilon_3$.

From Eq.(D.1) it follows that

$$\begin{aligned} V &= \gamma_0 + \gamma_2 x^2 - A(T_j)Sx + B(T_j)S = \bar{\gamma}_0 + \gamma_1 z + \bar{\gamma}_2 z^2, \\ \bar{\gamma}_0 &= \gamma_0 + B(T_j)S, \quad \gamma_1 = \frac{a_2}{b_2} A(T_j)S, \quad \bar{\gamma}_2 = \gamma_2 \frac{a_2^2}{b_2^2}. \end{aligned} \tag{D.3}$$

It was proven in Carr and Itkin (2018) that interpolation Eq.(D.1) preserves no-arbitrage, and so that in Eq.(D.3). We use it when computing $\mathcal{J}_2(x)$ in Eq.(84).

References

- Abramowitz, M., Stegun, I., 1964. Handbook of Mathematical Functions. Dover Publications, Inc.
- Askey, R., Daalhuis, A.B.O., 2010. Generalized hypergeometric function, in: Olver, F., Lozier, D., Boisvert, R., Clark, C. (Eds.), NIST Handbook of Mathematical Functions. Cambridge University Press.
- Balaraman, G., 2016. Modeling Volatility Smile and Heston Model Calibration Using QuantLib Python. Available at <http://gouthamanbalaraman.com/blog/volatility-smile-heston-model-calibration-quantlib-pyt>
- Bateman, H., Erdélyi, A., 1953. Higher Transcendental Functions. volume 1 of *Bateman Manuscript Project California Institute of Technology*. McGraw-Hill.
- Bergomi, L., 2016. Stochastic Volatility Modeling. CRC Financial Mathematics Series, Chapman and Hall.
- Bochner, S., 1949. Diffusion equation and stochastic processes, in: Proceedings of the National Academy of Sciences, USA, pp. 368–370.
- Carr, P., Itkin, A., 2018. An expanded local variance gamma model. Available at <https://arxiv.org/abs/1802.09611>.
- Carr, P., Nadtochiy, S., 2014. Local variance gamma and explicit calibration to option prices. Available at <https://arxiv.org/abs/1308.2326>.
- Carr, P., Nadtochiy, S., 2017. Local Variance Gamma and explicit calibration to option prices. *Mathematical Finance* 27, 151–193.
- Coleman, T., Kim, Y., Li, Y., Verma, A., 2001. Dynamic hedging with a deterministic local volatility function model. *The Journal of Risk* 4, 63–89.
- De Marco, S., Friz, P., Gerhold, S., 2013. Rational shapes of local volatility. *Risk* , 82–87.
- Derman, E., Kani, I., 1994. Riding on a smile. *RISK* , 32–39.
- Dupire, B., 1994. Pricing with a smile. *Risk* 7, 18–20.
- Ekström, E., Tysk, J., 2012. Dupire’s equation for bubbles. *International Journal of Theoretical and Applied Finance* 15, 1250041–1250053.
- Gatheral, J., 2006. The volatility surface. Wiley finance.

- Gerhold, S., Friz, P., 2015. Extrapolation analytics for Dupire's local volatility, in: *Large Deviations and Asymptotic Methods in Finance*. Springer. volume 110 of *Springer Proceedings in Mathematics & Statistics*, pp. 273–286.
- Hull, J., White, A., 2015. A generalized procedure for building trees for the short rate and its application to determining market implied volatility functions. *Quantitative Finance* 15, 443–454.
- Hull, J.C., 1997. *Options, Futures, and other Derivative Securities*. third ed., Prentice-Hall, Inc., Upper Saddle River, NJ.
- Itkin, A., 2015. To sigmoid-based functional description of the volatility smile. *North American Journal of Economics and Finance* 31, 264–291.
- Itkin, A., Lipton, A., 2018. Filling the gaps smoothly. *Journal of Computational Sciences* 24, 195–208.
- Kienitz, J., Caspers, P., 2017. *Interest Rate Derivatives Explained: Term Structure and Volatility Modelling*. volume 2 of *Financial Engineering Explained*. 1 ed., Palgrave Macmillan UK.
- Kienitz, J., Wetterau, D., 2012. *Financial Modelling: Theory, Implementation and Practice with MATLAB Source*. The Wiley Finance Series, Wiley.
- Lee, R., 2004. The moment formula for implied volatility at extreme strikes. *Mathematical Finance*. 14, 469–480.
- Lipton, A., 2001. *Mathematical Methods For Foreign Exchange: A Financial Engineer's Approach*. World Scientific.
- Lipton, A., Sepp, A., 2011. Credit value adjustment in the extended structural default model, in: *The Oxford Handbook of Credit Derivatives*. Oxford University, pp. 406–463.
- Lörinczi, J., Hiroshima, F., Betz, V., 2011. Feynman-Kac-Type Theorems and Gibbs Measures on Path Space. Number 34 in *De Gruyter Studies in Mathematics*, Walter de Gruyter GmbH & Co, Berlin/Boston.
- Ng, E., Geller, M., 1970. On some indefinite integrals of confluent hypergeometric functions. *Journal of research of the National Bureau of Standards - B. Mathematical Sciences* 74B, 85–98.
- Olver, F., 1997. *Asymptotics and Special Functions*. AKP Classics.
- Polyanin, A., Zaitsev, V., 2003. *Handbook of exact solutions for ordinary differential equations*. 2nd ed., CRC Press Company, Boca Raton, London, New York, Washington, D.C.

- Revuz, D., Yor, M., 1999. Continuous Martingales and Brownian Motion. 3rd ed., Springer, Berlin, Germany.
- Shreve, S., 1992. Martingales and the theory of capital-asset pricing. Lecture Notes in Control and Information SCIENCES 180, 809–823.
- Vasil'eva, A., Butuzov, V., Kalachov, L., 1995. The boundary function method for singular perturbation problems. Studies in Applied Mathematics, SIAM, Philadelphia.